Arachidonic acid inhibition of L-type calcium ($Ca_V1.3b$) channels varies with accessory $Ca_V\beta$ subunits

Mandy L. Roberts-Crowley and Ann R. Rittenhouse

Department of Physiology and Program in Neuroscience, University of Massachusetts Medical School, Worcester, MA 01655

Arachidonic acid (AA) inhibits the activity of several different voltage-gated Ca^{2+} channels by an unknown mechanism at an unknown site. The Ca^{2+} channel pore-forming subunit ($Ca_V\alpha_1$) is a candidate for the site of AA inhibition because T-type Ca^{2+} channels, which do not require accessory subunits for expression, are inhibited by AA. Here, we report the unanticipated role of accessory $Ca_V\beta$ subunits on the inhibition of $Ca_V1.3b$ L-type (L-) current by AA. Whole cell Ba^{2+} currents were measured from recombinant channels expressed in human embryonic kidney 293 cells at a test potential of −10 mV from a holding potential of −90 mV. A one-minute exposure to 10 µM AA inhibited currents with β_{1b}, β_3, or β_4 58, 51, or 44%, respectively, but with β_{2a} only 31%. At a more depolarized holding potential of −60 mV, currents were inhibited to a lesser degree. These data are best explained by a simple model where AA stabilizes $Ca_V1.3b$ in a deep closed-channel conformation, resulting in current inhibition. Consistent with this hypothesis, inhibition by AA occurred in the absence of test pulses, indicating that channels do not need to open to become inhibited. AA had no effect on the voltage dependence of holding potential–dependent inactivation or on recovery from inactivation regardless of $Ca_V\beta$ subunit. Unexpectedly, kinetic analysis revealed evidence for two populations of L-channels that exhibit willing and reluctant gating previously described for Ca_V2 channels. AA preferentially inhibited reluctant gating channels, revealing the accelerated kinetics of willing channels. Additionally, we discovered that the palmitoyl groups of β_{2a} interfere with inhibition by AA. Our novel findings that the $Ca_V\beta$ subunit alters kinetic changes and magnitude of inhibition by AA suggest that $Ca_V\beta$ expression may regulate how AA modulates Ca^{2+}-dependent processes that rely on L-channels, such as gene expression, enzyme activation, secretion, and membrane excitability.

INTRODUCTION

In the nervous system, voltage-gated L-type (L-) Ca^{2+} channels are composed of several proteins: the pore-forming $Ca_V\alpha_1$ subunit, through which Ca^{2+} ions pass, and accessory $Ca_V\beta$ and $\alpha_2\delta$ subunits (Catterall, 2000). Neurons in the brain express two isoforms of the L-channel $Ca_V\alpha_1$ subunit: $Ca_V1.2$ and $Ca_V1.3$ (Hell et al., 1993). The $Ca_V1.3$ isoform plays a role in gene expression (Gao et al., 2006; Zhang et al., 2006), exocytosis (Brandt et al., 2005), and membrane excitability (Brandt et al., 2003; Olson et al., 2005), depending on the cell type and localization.

L-channel activity is inhibited by signal transduction pathways downstream of neurotransmitters, including certain types of dopamine (Wikstrom et al., 1999; Banihashemi and Albert, 2002; Olson et al., 2005), glutamate (Chavis et al., 1994), serotonin (Cardenas et al., 1997; Day et al., 2002), and acetylcholine receptors (Pemberton and Jones, 1997; Bannister et al., 2002; Liu et al., 2006). Activation of these G protein–coupled receptors (GPCRs) also releases arachidonic acid (AA; C20:4) (Axelrod et al., 1988; Lazarewicz et al., 1992; Yehuda et al., 1998; Tang et al., 2006). Our laboratory has documented that endogenous AA release is necessary for muscarinic M1 receptor (M1) inhibition of L-current in superior cervical ganglion (SCG) neurons (Liu et al., 2006). Moreover, exogenously applied AA inhibits L-current in SCG neurons similarly to M_1R agonists (Liu et al., 2006). The $Ca_V1.3b$ L-channel isoform has been detected and cloned from SCG neurons (Lin et al., 1996), suggesting that endogenous AA modulates $Ca_V1.3b$.

The mechanism by which AA acts downstream of GPCR activation to inhibit L-current remains incompletely characterized. Single-channel recordings from SCG indicate that AA decreases the open probability of L-channels by increasing the dwell time in a closed state with no effect on unitary channel conductance (Liu and Rittenhouse, 2000). Similar findings of AA affecting closed states have been reported for the T-type (T-) Ca^{2+} channel, $Ca_V3.1$ (Talavera et al., 2004). A second family

Correspondence to Ann R. Rittenhouse:
Ann.Rittenhouse@umassmed.edu

Abbreviations used in this paper: AA, arachidonic acid; CTL, control; DHP, dihydropyridine; ETYA, 5,8,11,14-eicosatetraynoic acid; GPCR, G protein–coupled receptor; HEK, human embryonic kidney; L-, L-type; M1, muscarinic M1 receptor; O, open channel conformation; PA, palmitic acid; PIP_2, phosphatidylinositol-4,5-bisphosphate; RC, reluctant closed channel conformation; SCG, superior cervical ganglion; T-, T-type; TTP, time to peak; WC, willing closed channel conformation.

The Rockefeller University Press $30.00
J. Gen. Physiol. Vol. 133 No. 4 387–403
www.jgp.org/cgi/doi/10.1085/jgp.200810047

member, $Ca_V3.2$, is also inhibited by AA but via a leftward shift in holding potential–dependent inactivation (Zhang et al., 2000). Additionally, both T-channel studies reported increases in the rate of fast inactivation after AA, whereas our study on whole cell SCG L-current revealed no such changes (Liu et al., 2001). One obvious difference between T- and L-channels is that T-channels lack the recognition sequence in the I-II linker for binding $Ca_V\beta$ subunits (Arias et al., 2005), whereas $Ca_V\beta$ binding to L-channels fine-tunes their kinetics and voltage dependence of activation and inactivation (Singer et al., 1991; Hering et al., 2000; Kobrinsky et al., 2004). Whether certain $Ca_V\beta$ subunits block kinetic changes elicited by AA or whether $Ca_V1.3$ lacks a homologous site that confers the kinetic changes is unknown.

Therefore, to examine the extent of AA's actions on L-channel activity, we tested whether coexpression of $Ca_V1.3b$ with different $Ca_V\beta$ subunits accounts for the lack of kinetic changes observed by AA inhibition of whole cell L-current in SCG neurons. We show that AA inhibits $Ca_V1.3b$ currents expressed in human embryonic kidney (HEK) 293 cells by stabilizing channels in a closed state. Inhibition occurs regardless of which $Ca_V\beta$ subunit is coexpressed; however, the magnitude of inhibition produced and whether kinetic changes occur after AA depend on the $Ca_V\beta$ subunit. Physiologically, the tissue-specific expression of different $Ca_V\beta$ subunits is predicted to affect the response of L-channels after the stimulation of certain GPCRs or exposure to high levels of free AA, such as during ischemia.

MATERIALS AND METHODS

Cell culture

The HEK cell line, stably transfected with the M1 muscarinic receptor (HEK M1; provided by E. Liman, University of Southern California, Los Angeles, CA, and originally transfected by Peralta et al., 1988) was propagated at 37°C with 5% CO_2 in Dulbecco's MEM (DMEM)/F12 supplemented with 10% FBS, 1% G418, 0.1% gentamicin, and 1% HT supplement (Invitrogen). Cells were passaged once they became 80% confluent.

Transfection

HEK M1 cells were placed in 12-well plates at ~60–80% confluence and transfected with a 1:2:1 molar ratio of $Ca_V1.3b$, $Ca_V\beta$, and $\alpha_2\delta$-1 subunits (Xu and Lipscombe, 2001) using Lipofectamine PLUS (Invitrogen) according to the manufacturer's instructions. Constructs for $Ca_V1.3b$ (+exon11, Δexon32, and +exon42a; GenBank accession no. AF370009), $Ca_V\beta_3$ (no. M88751), and $\alpha_2\delta$-1 (no. AF286488) were provided by D. Lipscombe (Brown University, Providence, RI). Constructs for $Ca_V\beta_{1b}$ (GenBank accession no. X61394), $Ca_V\beta_{2a}$ (no. M80545), and $Ca_V\beta_4$ (no. L02315) were provided by E. Perez-Reyes (University of Virginia, Charlottesville, VA). $Ca_V\beta_{2a}$ C3,4S was constructed by M. Hosey's lab (Chien et al., 1996) and supplied by A. Fox (University of Chicago, Chicago, IL). The $Ca_V\beta_{2e}$ (AF423192) construct was provided by H.M. Colecraft (Columbia University, New York, NY), and the $Ca_V\beta_{2a}$C3,4S-CD8 construct was provided by P. Charnet (Centre National de la Recherche Scientifique, Paris, France). For all transfections, 0.5 µg DNA was used per well of a 12-well plate. Green fluorescent protein cDNA was <10% of the total cDNA used. Cells were washed with DMEM, and the DNA mixture was added dropwise to each well, gently rocked, and then incubated for 1 h at 37°C in a 5% CO_2 incubator. Supplemented media, without antibiotics, was returned to the cells to bring the volume up to 1 ml (normal growth medium volume). After 2 h, cells were washed with full media. Cells were washed a final time 2 h later, and 10 mM $MgSO_4$ was added. Cells were transferred 24–72 h after transfection using 2 mM EDTA in 1× PBS to poly-L-lysine–coated coverslips; recording began 1 h after transfer.

Electrophysiology

Electrodes were pulled from borosilicate glass capillary tubes (Drummond Scientific Company). Each electrode tip was fire polished to a diameter of ~1 µm to give the pipette a resistance of 2–4 MΩ. Whole cell currents were recorded at room temperature (20–24°C) with an Axon 200B patch clamp amplifier (MDS Analytical Technologies). Currents were filtered at 5 or 20 kHz and digitized at five times the filter cut-off frequency of the four-pole Bessel filter. Data were acquired using Signal software (Cambridge Electronic Design) and stored for later analysis on a personal computer. For time course experiments, a holding potential of −60 or −90 mV was used, and currents were measured at a test potential of −10 mV for 40 ms at 5-s intervals. For holding potential–dependent inactivation experiments, a holding potential of −60 mV was used and the "conditioning" potential varied from −100 to +50 mV for 2.2 s, immediately followed by a test potential of −10 mV for 40 ms.

The pipette solution consisted of (in mM): 125 Cs-aspartate, 10 HEPES, 0.1 BAPTA, 5 $MgCl_2$, 4 ATP, and 0.4 GTP brought to pH 7.50 with CsOH. High resistance seals were established in Mg^{2+} Tyrode's consisting of (in mM): 5 $MgCl_2$, 145 NaCl, 5.4 KCl, and 10 HEPES brought to pH 7.50 with NaOH. Once a seal was established and the membrane ruptured, the Tyrode's solution was exchanged for an external bath solution consisting of (in mM): 125 NMG-aspartate, 20 Ba^{2+}, and 10 HEPES brought to pH 7.50 with CsOH. AA (all-*cis* 5,8,11,14-eicosatetraynoic acid; NuCheck Prep), oleic acid (NuCheck Prep), and ETYA (BioMol) were dissolved in 100% EtOH and stored under nitrogen as stock solutions at −70°C. Working dilutions were made fresh daily by diluting stock solutions at least 1:1,000 in external bath solution. A final concentration of 10 µM AA was used unless otherwise noted. Palmitic acid (PA) was prepared daily as a 50-mM stock solution in EtOH and diluted to a final concentration of 10 µM in external bath solution. BSA (fraction V, heat shock, fatty acid ultra-free; Roche) was diluted 1 mg/ml directly in bath solution. All chemicals were purchased from Sigma-Aldrich unless otherwise noted.

Data analysis

Linear leak and capacitive currents were subtracted and maximal inward current amplitudes were measured after the onset of the test pulse (peak current). Percent inhibition was calculated as

$$\%I_{Inhib} = 100*(I_{CTL} - I_{INHIB})/I_{CTL},$$

where I_{CTL} is the average of five peak inward current values before the application of test material, and I_{INHIB} is the average of five peak inward current values 1 min after the application of test material (unless otherwise noted). Difference current was measured as

$$I_{Difference} = I_{CTL} - I_{INHIB}.$$

Time to peak (TTP) was measured using a trough-seeking function in Signal within the test pulse duration. Current remaining was measured from an average of five individual sweeps per recording using the equation:

$$I_R = 100*(I_{END}/I_{PEAK}),$$

where I_R is the current remaining at the end of a 40-ms ($r40$) or 2.2-s ($r2200$) test pulse, I_{END} is the value at the end of the test pulse, and I_{PEAK} is the maximum inward current measured during the test pulse. Conductance was calculated from a modified Ohm's Law equation:

$$G = I_{PEAK} / (V_m - V_{rev}),$$

where I_{PEAK} is the peak current at each test potential, V_m is the test potential, and V_{rev} is the reversal potential. Relative conductance (G/G_{max})-voltage (V_m) curves were plotted and fit using the Boltzmann equation:

$$G/G_{max} = G_{max} + (G_{min} - G_{max})/[1 + exp(V_m - V_m1/2)/k],$$

where G_{max} is the maximal conductance, G_{min} is the minimal conductance, V_m is the test potential, $V_m1/2$ is the voltage at half-maximal conductance, and k is the slope factor. Holding potential–dependent inactivation was plotted as normalized current during the test pulse against the conditioning pulse voltage. The inactivation curve was fit using the Boltzmann equation:

$$I/I_{max} = I_{max} + (I_{min} - I_{max})/[1 + exp(V_m - V_{inact}1/2)/k],$$

where V_m is the conditioning pulse and $V_{inact}1/2$ is the voltage where half the maximal number of channels has inactivated. The rate of inactivation was measured by fitting the current traces to a biexponential function yielding time constants for a fast (τ_{fast}) and slow (τ_{slow}) component:

$$I = A_{fast}^{(-t/\tau fast)} + A_{slow}^{(-t/\tau slow) + A0},$$

where A_{fast} and A_{slow} are the current amplitudes with the respective time constants, and A_0 is any remaining current. The time courses for recoveries from fast and slow inactivation were fit to the same biexponential function yielding time constants for τ_{fast} and τ_{slow} components.

Statistical analysis

Data are presented as mean values ± SEM. Data were analyzed statistically using either a one-way ANOVA followed by a Tukey multiple comparison post-hoc test or a two-tailed paired or unpaired Student's *t* test. Statistical significance was set at $P \leq 0.05$. Analysis programs included Signal (Cambridge Electronic Design), Excel (Microsoft), and Origin (OriginLab).

Online supplemental material

Fig. S1 shows that 10 μM oleic acid had no significant effect on β2a- and β3-containing channels. Fig. S2 shows that no significant correlations among control current amplitude, control $r40$, and percent inhibition by 10 μM AA were found for $Ca_V1.3$ currents coexpressed with any of the β-subunits. Correlations were calculated for recordings using a holding potential of −90 or −60 mV. Fig. S3 shows that rate of activation is faster in the presence of AA when fitting current traces to the equation: $I_{Ba} = A_0 e^{(-t/t_1)}$. $Ca_V1.3$ currents, regardless of the $Ca_V\beta$ subunit coexpressed, were best fitted to one exponential. Figs. S1–S3 are available at http://www.jgp.org/cgi/content/full/jgp.200810047/DC1.

RESULTS

AA inhibits $Ca_V1.3b$ L-Ca^{2+} currents regardless of the $Ca_V\beta$ subunit

To determine if AA inhibits $Ca_V1.3b$ activity, peak current amplitudes were measured from −90 mV to a test pulse of −10 mV every 5 s before and after the application of 10 μM AA to cells transiently transfected with $Ca_V1.3b$, β_3, $\alpha_2\delta$-1, and green fluorescent protein. AA produced a 51 ± 8% inhibition of current after 1 min ($n = 7$; $P < 0.001$). We then tested whether inhibition occurred in a concentration-dependent manner and found that the magnitude of inhibition increased with increasing AA concentration (Fig. 1, A and B). To stay well below the critical micelle concentration, concentrations >10 μM AA were not tested. In measuring current inhibition, we noticed an apparent acceleration in activation kinetics that was most pronounced with 10 μM AA (Fig. 1 B) and was apparent when current traces were normalized to the end of the 40-ms test pulse (Fig. 1 C). The increased rate of activation (Fig. 1 D, top), measured as TTP, maximally decreased after 1 min, whereas current inhibition (Fig. 1 D, bottom) developed over the span of 3 min. The application of 1 mg/ml BSA, which binds free fatty acid, reversed both the kinetic changes and current inhibition, indicating that channels were specifically modulated as opposed to nonspecific rundown of channel activity over time.

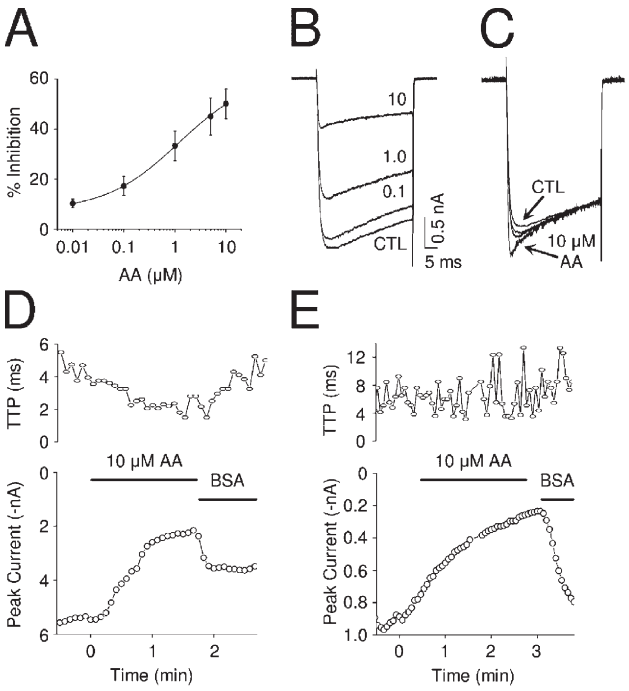

Figure 1. AA modulates amplitude and kinetics of whole cell $Ca_V1.3b$ currents. (A) Concentration–response curve of AA on $Ca_V1.3b$, β_3 currents. Concentrations of 0.01, 0.1, 1, 5, and 10 μM were bath applied, and current inhibition was measured after 1 min (n = 3–11). (B) Individual traces of $Ca_V1.3b$, β_3 currents before (CTL) and after the application of 0.1, 1, or 10 μM AA. (C) Individual traces from B were normalized, revealing that exposure to 10 μM AA decreases the TTP. (D) TTP and current amplitude for $Ca_V1.3b$, β_3 currents plotted versus time. Bars indicate where 10 μM AA and 1 mg/ml BSA were added. Both changes reverse after wash with BSA. (E) TTP and current amplitude for $Ca_V1.3b$, β_{2a} currents plotted versus time. Conditions are the same as in D. No TTP change is observed. AA still inhibits current over time that reversed by washing with BSA.

The change in TTP was unanticipated because native L-current in SCG neurons exhibits no apparent kinetic change when inhibited by AA (Liu et al., 2001). Additionally, whole cell L-current in SCG neurons is non-inactivating as opposed to the relatively rapid inactivating current observed with unmodulated transfected $Ca_V1.3b$, β_3 currents (Fig. 1 B, control [CTL]). Non-inactivating current kinetics are characteristic of channels associated with β_{2a}, which is uniquely palmitoylated, tethering it to the membrane and conferring different inactivation properties (Chien et al., 1996). Therefore, we tested whether the AA-induced TTP change also occurs with β_{2a}. Fig. 1 E (bottom) shows that 10 μM AA significantly inhibited current from cells transfected with $Ca_V1.3b$, $\alpha_2\delta$, and β_{2a} by 31 ± 7% after 1 min (n = 8; $P < 0.001$). However, no change in TTP was observed (Fig. 1 E, top). After 3 min, current was inhibited by 56 ± 15% (n = 5; $P < 0.001$), suggesting that currents from β_{2a}-containing channels can be inhibited to a similar extent as β_3-containing channels after 1 min. The application of BSA recovered inhibited current. These differences suggest that different $Ca_V\beta$ subunits uniquely tune $Ca_V1.3b$ modulation by AA.

Four genes in the $Ca_V\beta$ family (β_1, β_2, β_3, and β_4) and several splice variants have been identified to date (Birnbaumer et al., 1998; Takahashi et al., 2004). To test the effects of other $Ca_V\beta$ family members on the modulation of $Ca_V1.3b$ by AA, we compared representative current traces for $Ca_V1.3b$ currents coexpressed with β_{1b}, β_{2a}, β_3, or β_4 in the absence (CTL) or presence of 10 μM AA (Fig. 2 A). After a 1-min exposure to AA, the magnitude of inhibition was 58 ± 6% for β_{1b} (n = 7; $P < 0.001$) and 44 ± 4% for β_4 (n = 6; $P < 0.001$) (Fig. 3 A). Thus, AA inhibits $Ca_V1.3b$ regardless of the $Ca_V\beta$ subunit coexpressed, but the magnitude of inhibition is less for β_{2a} and is not accompanied by kinetic changes. The finding that β_{2a}-containing channels exhibit a profile of modulation identical to our studies of native L-current (Liu et al., 2001) suggests that $Ca_V1.3$ in SCG neurons primarily couples to β_{2a}.

To visualize differences in kinetics, individual traces were normalized to the end of the 40-ms test pulse (Fig. 2 B). When the inhibited current was subtracted from CTL current, the difference current revealed a relatively non-inactivating shape for currents with each of the $Ca_V\beta$ subunits (Fig. 2 C). The loss of non-inactivating current after AA is similar to whole cell difference currents recorded in SCG neurons and is consistent with AA-stabilizing channels in closed or inactivated states, thus removing inhibited channels from contributing to the whole cell current. This result suggests that the current actually inhibited by AA inactivates very little, whereas the residual current displays more inactivation for β_{1b}-, β_3-, or β_4-containing channels.

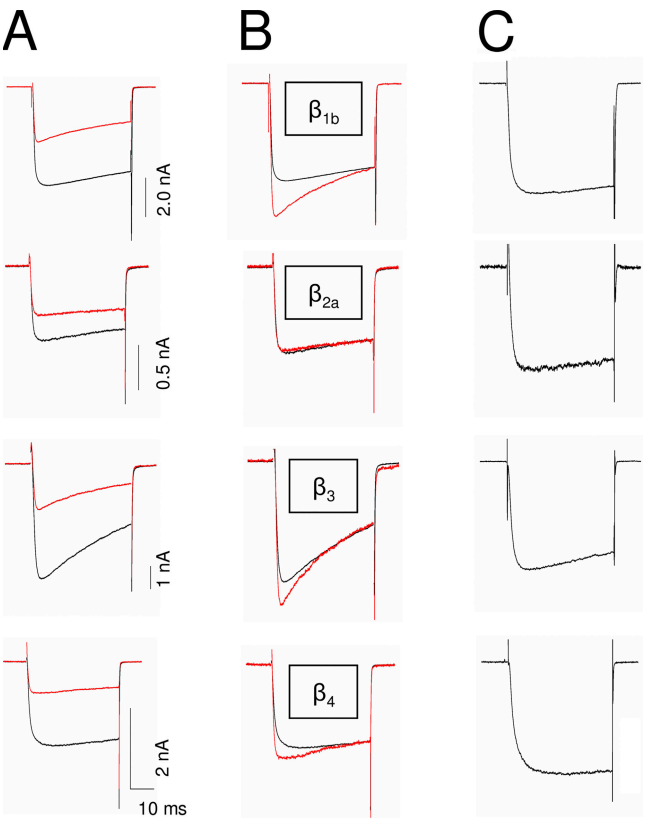

Figure 2. $Ca_V1.3b$ current inhibition and kinetic changes by AA are $Ca_V\beta$ subunit dependent. (A) Representative current traces from $Ca_V1.3b$ channels coexpressed with β_{1b}, β_{2a}, β_3, or β_4 before (CTL; black line) or 1 min after AA (10 μM; red line) application highlight the smaller amount of inhibition with β_{2a}. (B) Current traces from A were normalized to the end of the test pulse to highlight kinetic changes produced by AA for β_{1b}-, β_3-, and β_4-, but not β_{2a}-containing channels. (C) Inhibited currents were averaged and subtracted from averaged CTL currents to obtain a difference current for $Ca_V1.3b$ with each $Ca_V\beta$ subunit to determine the shape of the current lost after AA application (n = 7–13).

AA inhibits $Ca_V1.3b$ channels in deep closed states

Single-channel analysis of L-current inhibition by AA revealed an increase in null sweeps and a decrease in open probability (Liu and Rittenhouse, 2000), suggesting that AA increases the number of channels dwelling in a non-conducting conformation: either closed or inactivated. Additionally, first latency, the time for a single channel to transition from closed to open in response to a test pulse, increases from ~30 to 90 ms (Liu and Rittenhouse, 2000), indicating that when an L-channel is affected by AA, the time to transition from closed to open increases. These results support a model where AA stabilizes a closed conformation rather than an inactivated conformation because inactivated channels will not respond to voltage until sufficient time has transpired for channels to recover.

Many kinetic models display closed Ca^{2+} channels in at least four closed conformations representing the movement of each voltage sensor from domains I–IV of the

$Ca_V\alpha_1$ subunit in response to changes in membrane potential to the open conformation (Patil et al., 1998; Serrano et al., 1999). For example, at a holding potential of −90 mV, none of the voltage sensors have moved and channels reside primarily in a deep closed state (Marks and Jones, 1992); at a holding potential of −60 mV, the voltage sensors have moved in response to depolarization and channels reside in closed conformations closer to the open state. Therefore, we tested whether holding cells at −60 mV would alter the magnitude of $Ca_V1.3b$ inhibition by AA compared with holding cells at −90 mV. AA suppressed $Ca_V1.3b$ currents with β_{1b}, β_3, or β_4 by 34 ± 6%, 26 ± 7%, or 26 ± 4%, respectively (Fig. 3 B), but with β_{2a}, only by 12 ± 6% (n = 7–13; $P < 0.001$ for all $Ca_V\beta$ subunits compared with CTL; $P < 0.05$ for all $Ca_V\beta$ subunits comparing current inhibition from −90 to −60 mV). From −60 mV, TTP continued to be unaffected by AA application for channels with β_{2a} and decreased for channels with β_3 (Fig. 3 C). Overall, current inhibition by AA was greater for all $Ca_V\beta$ subunits recorded with a holding potential of −90 mV than with −60 mV, consistent with AA stabilizing a deep closed state (Liu and Rittenhouse, 2000).

Next, we examined whether channels need to enter the open conformation for AA inhibition of $Ca_V1.3b$ currents. Here, we used a protocol with short 10-ms test pulses and no depolarization for 1 min in the absence or presence of AA (Fig. 3 D). The protocol was designed to maintain channels in a closed conformation; the shorter test pulse should minimize the amount of inactivation. Additionally, no depolarization for 1 min should bring channels into a resting, closed conformation. The 10-ms test pulse from −60 mV had no effect on the ability of AA to inhibit currents from β_3-containing channels. In fact, the shorter 10-ms test pulse showed more inhibition after 1 min (35%; Fig. 3 E) than recordings with 40-ms test pulses (26%; Fig. 3, B and E). In the absence of test pulses, AA inhibited 34% of the current (n = 7; $P <$ 0.001 compared with CTL current before the application of AA). Moreover, BSA reversed inhibition to CTL peak amplitudes (not depicted). Overall, these experiments suggest that $Ca_V1.3b$ does not need to open to become inhibited by AA.

ETYA mimics the inhibitory profile of $Ca_V1.3b$ by AA

To address the specificity of AA inhibition and the possible role of AA metabolites, a nonhydrolyzable form of AA, ETYA, was tested for inhibition of $Ca_V1.3b$ currents. From a holding potential of −60 mV, current was measured 1 min after the application of 30 µM ETYA. Fig. 4 A shows representative individual sweeps for each of the $Ca_V\beta$ subunits before or after ETYA. To visualize differences in kinetics, individual traces were normalized to the end of the 40-ms test pulse (Fig. 4 B). ETYA inhibited currents for β_{1b}-, β_{2a}-, β_3-, or β_4-containing channels 32 ± 8%, 14 ± 4%, 24 ± 5%, or 22 ± 6%, respectively

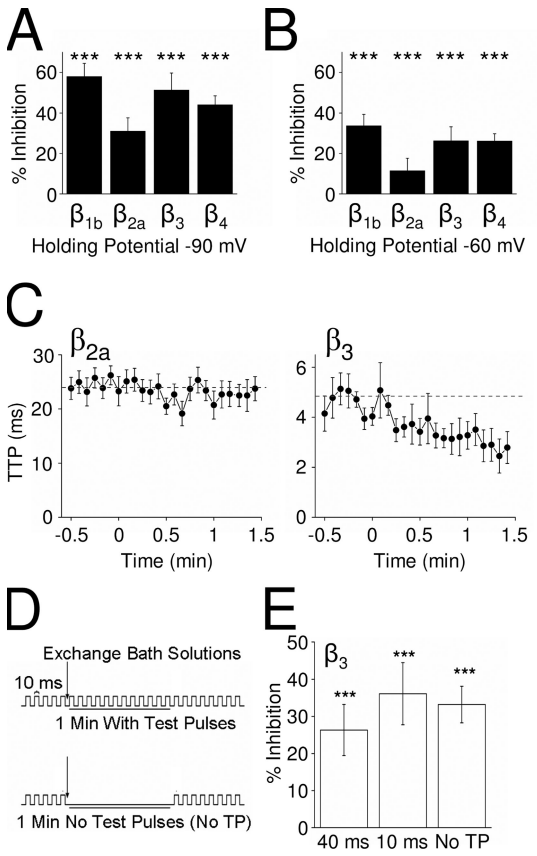

Figure 3. AA inhibition stabilizes closed states of $Ca_V1.3b$. (A and B) Summary of average percent inhibition of $Ca_V1.3b$ currents after a 1-min exposure to 10 µM AA from a holding potential of −90 mV (A) or −60 mV (B; n = 7–17; ***, $P < 0.001$ compared with CTL currents and $P < 0.05$ comparing percent inhibition by AA at −90 to −60 mV for all β subunits). (C) Time course of averaged TTP for $Ca_V1.3b$ currents with β_{2a} (left) or β_3 (right) from a holding potential of −60 mV. (D) Protocol for studying AA inhibition in the absence of depolarizing test pulses (TP) from a holding potential of −60 mV. (E) Summary bar graph for percent inhibition by AA: left, with 40-ms test pulses; middle, with 10-ms test pulses; right, with no test pulses (n = 5–7; ***, $P < 0.001$ compared with CTL currents).

(n = 5–8; $P < 0.001$ compared with CTL) (Fig. 4 C). ETYA inhibition did not significantly differ from AA inhibition from a holding potential of −60 mV shown in Fig. 3 B (β_{1b}, $P \geq 0.89$; β_{2a}, $P \geq 0.81$; β_3, $P \geq 0.78$; β_4, $P \geq 0.59$). To test whether the effects of ETYA and AA were additive, 30 µM ETYA was added for 1 min, 30 µM ETYA + 10 µM AA was added for another minute, and current inhibition was measured. Current was further inhibited by ETYA + AA for a total inhibition of 49 ± 7% (n = 4; $P <$ 0.001 compared with CTL; $P < 0.05$ compared with ETYA alone) for $Ca_V1.3b$ currents with β_3. This magnitude of inhibition is similar to that measured by 10 µM AA alone after application for 2 min (not depicted). These results suggest that inhibition is the result of AA itself and not a metabolite. In contrast to polyunsaturated AA or ETYA, 10 µM oleic acid (C18:1), a monounsaturated fatty acid, had no significant effect on currents

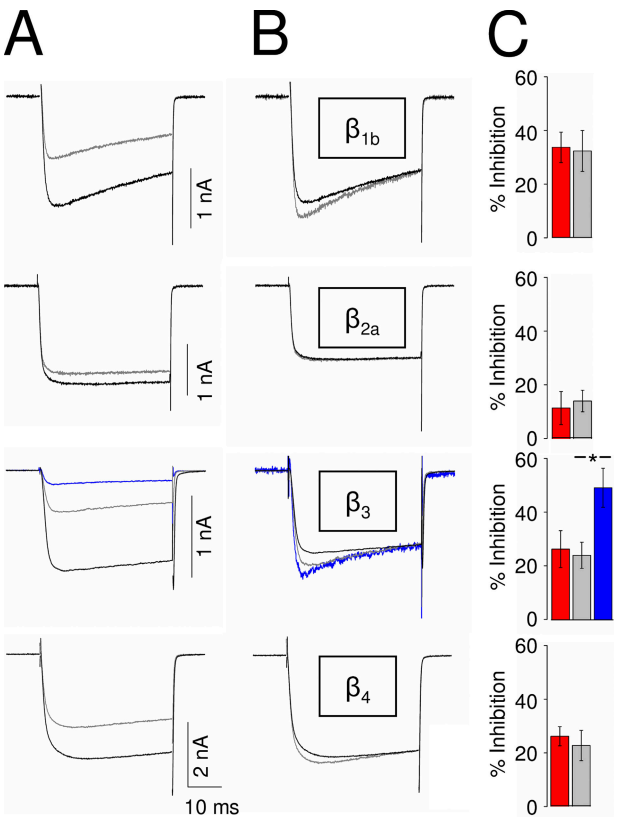

Figure 4. ETYA mimics the inhibition profile of AA with different $Ca_V\beta$ subunits. Inhibition was measured 1 min after the application of 30 µM ETYA from a holding potential of −60 mV. (A) Representative traces for $Ca_V1.3b$ currents with β_{1b}, β_{2a}, β_3, or β_4 in the absence (CTL; black line) and presence of 30 µM ETYA (gray line) or 30 µM ETYA + 10 µM AA (blue line, for β_3). (B) Normalized representative traces from A. (C) Summary bar graphs of percent inhibition (n = 5–8). No statistical difference occurred with percent inhibition at 1 min by ETYA (gray bars) compared with AA (red bars; from Fig. 3 B). For $Ca_V1.3b$, β_3 currents, ETYA was bath applied for 1 min, and then ETYA + AA was added for another minute (blue bar; n = 4; *, P < 0.05).

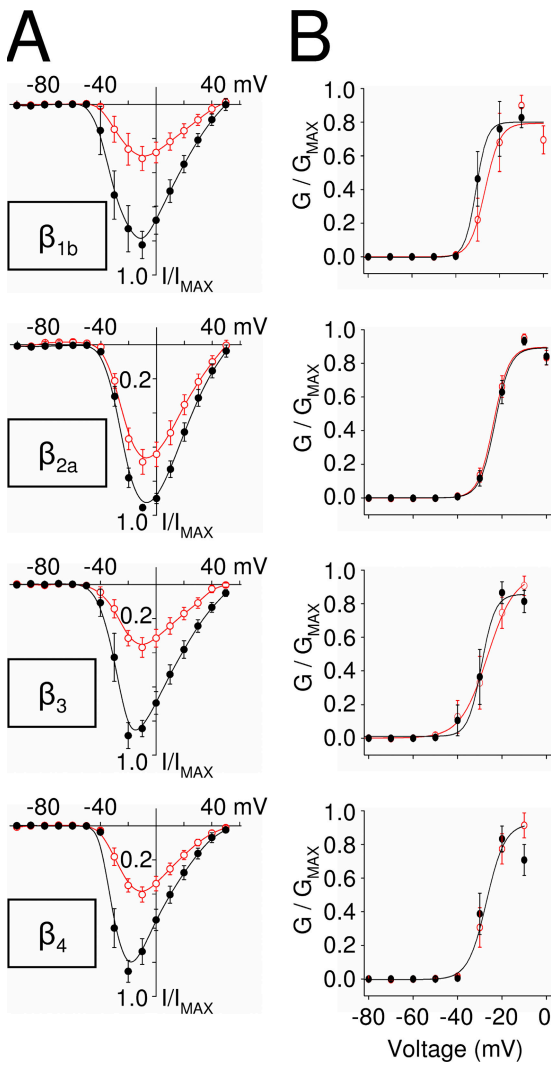

Figure 5. $Ca_V1.3b$ inhibition by AA is not due to a shift in voltage-dependent activation. (A) I-V curves from CTL currents (filled circle, black line) or after a 1-min exposure to 10 µM AA (open circle, red line). I-V curves were normalized to peak CTL current for each recording and then averaged (n = 7–13). (B) G-V curves measured from A.

from channels containing β_{2a} (n = 4; P ≥ 0.66) or β_3 (n = 3; P ≥ 0.58) (Fig. S1), indicating that inhibition requires certain aspects of fatty acid structure.

Inhibition of $Ca_V1.3b$ by AA is not due to a shift in voltage sensitivity

To thoroughly analyze any changes in the overall closed to open transitions, we examined the effect of AA on peak current over a range of test potentials (−100 mV to +50 mV in 10-mV steps). In I-V plots, all currents, regardless of the $Ca_V\beta$ subunit expressed with $Ca_V1.3b$, activated at −50 mV, peaked at −10 mV, and reversed at +50 mV, similar to previous reports of $Ca_V1.3$ activating at low voltages (Koschak et al., 2001; Xu and Lipscombe, 2001). AA inhibited currents at all voltages regardless of the $Ca_V\beta$ subunit (Fig. 5 A). G-V plots revealed no shift in the activation curve by AA compared with CTL plots (Fig. 5 B), consistent with inhibited channels becoming unavailable to open (stabilized closed) and thus not contributing to the G-V relationship. Therefore, AA inhibition is not the result of altering the voltage sensitivity of $Ca_V1.3b$.

$Ca_V1.3b$ kinetic changes with AA are not due to a shift in voltage sensitivity

Because these initial measurements are consistent with a model where AA stabilizes a deep closed state, we next sought to understand the observed changes in activation and inactivation described in Figs. 1 and 2. We first quantified current remaining at the end of the 40-ms test pulse (r40), respectively, for $Ca_V1.3b$ with each $Ca_V\beta$ subunit. For currents elicited from a holding potential of −90 to −10 mV, r40 (Fig. 6 A) significantly decreased after a 1-min exposure to AA for currents containing β_{1b}, β_3, or β_4, but not β_{2a} (n = 6–8; P < 0.05 for β_{1b}, β_3,

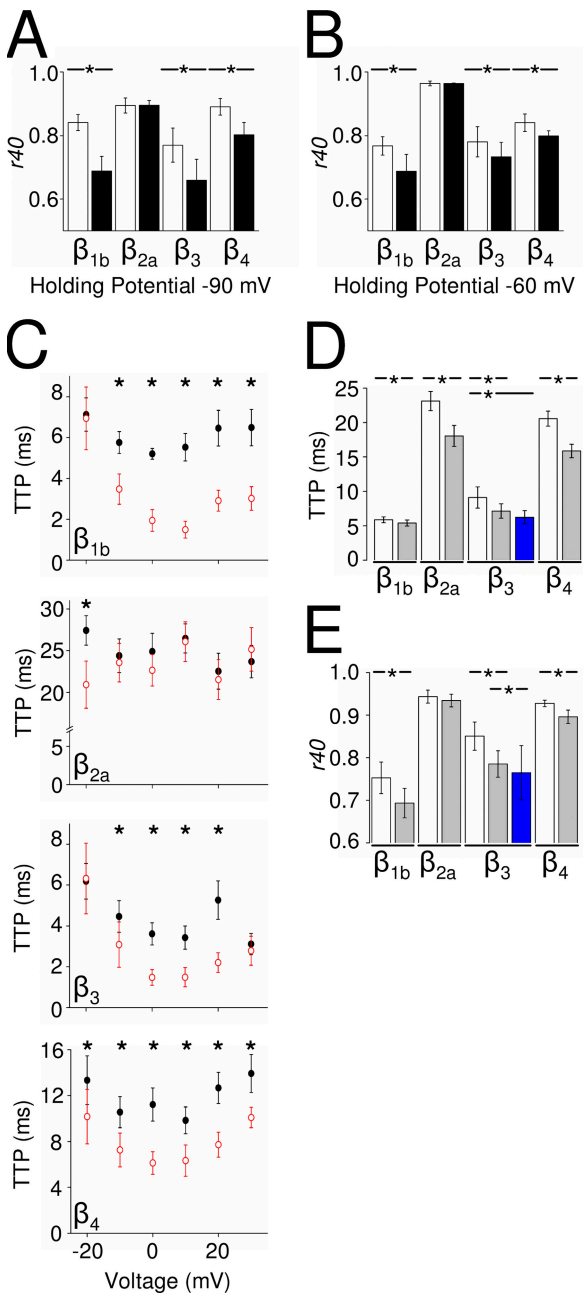

Figure 6. $Ca_V1.3b$ kinetic changes by AA are not due to a shift in voltage sensitivity. (A and B) Summary of average current remaining at the end of a 40-ms test pulse ($r40$) for currents before (open bars, CTL) or after a 1-min exposure to 10 µM AA (filled bars) from a holding potential of −90 mV (A) or −60 mV (B; n = 7–17; *, P < 0.05). (C) TTP for CTL (filled circles) or AA (open circles) currents across voltages where channels are activated from a holding potential of −60 mV (n = 7–13; *, P < 0.05). (D) Summary of TTP changes produced by 30 µM ETYA (open bars, CTL before ETYA; gray bars, 1 min after ETYA; blue bar, 1 min after 30 µM ETYA + 10 µM AA for β_3; n = 4–8; *, P < 0.05). (E) Summary of $r40$ changes produced by ETYA. Bar descriptions are the same as in D.

and β_4; P ≥ 0.48 for β_{2a}). Although less inhibition by AA was observed at −10 mV from a holding potential of −60 mV, the decrease in $r40$ was still apparent for channels with β_{1b}, β_3, and β_4; no kinetic changes were observed for channels with β_{2a} (n = 7–13; P < 0.05 for β_{1b}, β_3, and β_4; P ≥ 0.48 for β_{2a}) (Fig. 6 B). BSA reversed both the kinetic change and current inhibition regardless of holding potential (not depicted). Additionally, we found no correlations between CTL current amplitude, CTL $r40$, or percentage of AA-induced inhibition of $Ca_V1.3b$ with any $Ca_V\beta$ subunit (Fig. S2).

TTP was also measured across a range of test potentials from a holding potential of −60 mV. After AA application, TTP was generally faster for β_{1b}-, β_3-, or β_4-containing channels across voltages (Fig. 6 C). In contrast, TTP for $Ca_V1.3b$ with β_{2a}, which is slower than with the other $Ca_V\beta$ subunits, was only faster in the presence of AA at −20 mV. To confirm these data, activation time constants were measured at multiple test potentials before and after 1 min of AA (Fig. S3). The activation of $Ca_V1.3b$ was best fitted with one exponential (τ_{ACT}) for all $Ca_V\beta$ subunits, similar to previous monoexponential fits of $Ca_V1.3$ with β_3 (Koschak et al., 2001). The τ_{ACT} for $Ca_V1.3b$, β_{2a} currents was approximately threefold slower than that for the other $Ca_V\beta$ subunits. Overall, AA decreased the mean τ_{ACT} across voltages for $Ca_V1.3b$ currents with all $Ca_V\beta$ subunits, consistent with the decrease in TTP after AA. TTP kinetic changes were also apparent after AA with the shorter 10-ms test pulses (not depicted). These findings suggest that although the kinetic changes observed with β_{1b}-, β_3-, or β_4-containing channels occur with inhibition over the range of voltages tested, the TTP change produced by AA is not the result of a shift in voltage dependence of activation.

Kinetic changes produced by AA were also mimicked by ETYA. When comparing CTL currents to currents exposed to ETYA, TTP significantly decreased for all $Ca_V\beta$ subunits (n = 5–8; P < 0.05) (Fig. 6 D). Significant decreases in $r40$ were also observed for $Ca_V1.3b$ with β_{1b}, β_3, and β_4, but not with β_{2a} (Fig. 6 E). For $Ca_V1.3$ with β_3, TTP and $r40$ significantly decreased for ETYA + AA compared with CTL, but it did not significantly differ from ETYA alone. Thus, in addition to inhibition, the kinetic changes observed after AA application are not produced by an AA metabolite.

At least two explanations may account for the kinetic changes and the decrease in current amplitude after AA. In the first scenario, after exposure to AA, all of the channels shift to more reluctant gating where a greater voltage step is required to open channels. If this is the case, the activation curve will exhibit a rightward shift to more positive voltages after AA. Moreover, if AA shifts all channels toward reluctant gating, we would expect to observe a slower TTP. This scenario seems unlikely because no shift in the G-V curve occurs (Fig. 5 B), and TTP is faster at −10 mV in the presence of AA compared

with CTL currents, despite our previous findings that AA increases dwell times in closed conformations and increases first latency to 90 ms (Liu and Rittenhouse, 2000). Because the test pulse duration for the whole cell current recordings was 40 msec, the inhibited channels are unlikely to open.

In a second scenario, at least two populations of L-channels are present under CTL conditions: one population of channels is reluctant to open (reluctant closed channel conformation [RC]), whereas another population is willing to open (willing closed channel conformation [WC]), with the RC transition time to the open channel conformation (O) slower than the WC→O transition time (Jones and Elmslie, 1997). This description of reluctant gating has been described previously for Ca_V2 channels modulated by G proteins (Bean, 1989) or by phosphatidylinositol-4,5-bisphosphate (PIP_2) binding (Wu et al., 2002). CTL TTP can be expressed as the sum of RC→O plus WC→O transition times. After AA, a greater percentage of channels reside in the RC conformation longer and, therefore, will not open during the 40-ms test pulse due to the observed first latency increase to 90 ms (Liu and Rittenhouse, 2000). Consequently, the residual current displays only the faster WC→O transition. This model is consistent with the decreased TTP after AA. Similarly, RC channels show slower inactivation. Therefore, if RC channels are inhibited and WC channels remain active, an apparent increase in inactivation would occur. This model fits the observed kinetic changes in TTP and *r*40 after AA.

AA accentuates $Ca_V\beta$ subunit-dependent inactivation of $Ca_V1.3b$ currents

This simple model predicts that AA would only need to stabilize one or more deep closed states to confer the observed changes in channel gating; no change in fast or slow inactivation need occur. The above data rule out changes in fast inactivation. Therefore, we tested whether AA changes slower forms of inactivation. To test AA's effect on holding potential–dependent inactivation, a protocol was used in which channels were exposed to a series of "conditioning pulses" ranging from −100 to +50 mV (in 10-mV steps) for 2.2 s, and then repolarized to the test potential of −10 mV for 40 ms. Representative current traces for $Ca_V1.3$ with β_{2a} (Fig. 7, A and C) or β_3 (Fig. 7, B and D) are shown before (CTL) or after exposure to AA for 1 min. The long, 2.2-s conditioning pulse highlights the striking differences in inactivation kinetics between β_{2a}- and β_3-containing channels. Inactivation currents for $Ca_V1.3$ with β_{1b}, β_3, or β_4 were best fit with two exponentials ($\tau_{INACT\text{-}fast}$ and $\tau_{INACT\text{-}slow}$), whereas $Ca_V1.3$ β_{2a} currents were best fit with one exponential ($\tau_{INACT\text{-}slow}$). Fits of inactivation are shown overlying the representative traces (Fig. 7, C and D). Fig. 8 (A and B) summarizes the inactivation time constants for voltages from −20 to +40 mV. AA significantly decreased $\tau_{INACT\text{-}fast}$ at positive test potentials (0 to +40 mV)

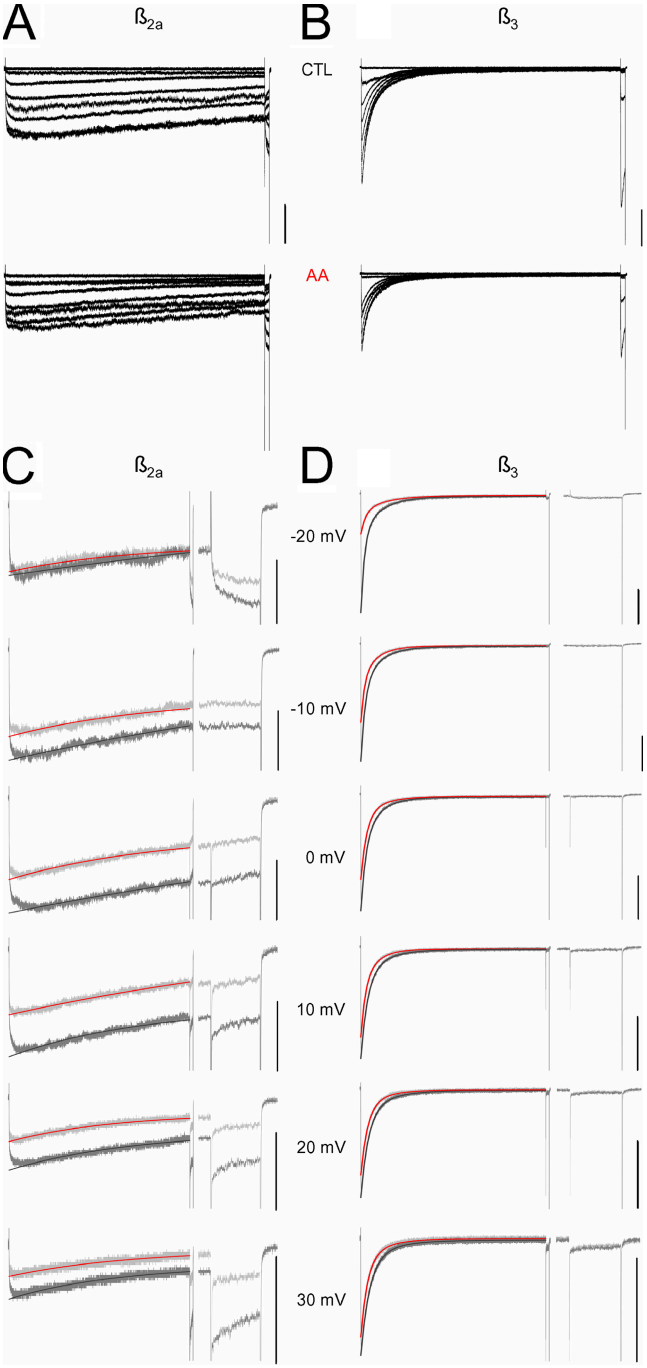

Figure 7. AA does not effect holding potential–dependent inactivation of $Ca_V1.3b$ currents. (A) Representative current traces from $Ca_V1.3b$, β_{2a} channels for CTL conditions (top) or 1 min after a 10 μM AA application (bottom) from a holding potential of −60 mV to conditioning pulses from −40 to +30 mV for 2.2 s, and then to a test pulse at −10 mV for 40 ms. Bar, 0.2 nA. (B) Representative current traces from $Ca_V1.3b$, β_3 channels. Conditions are similar to A. Bar, 0.5 nA. (C) Representative current traces from $Ca_V1.3b$, β_{2a} channels for CTL (gray) or inhibited currents 1 min after a 10-μM AA application (light gray) for 2.2-s conditioning pulses from −20 to +30 mV. Fits of inactivation overlay each trace (dark gray, CTL; red, AA). The 40-ms test pulse after the conditioning pulse is expanded on the right. Bar, 0.2 nA. (D) Representative current traces from $Ca_V1.3b$, β_3 channels. Conditions are similar to C. Bar, 0.5 nA.

for β_{1b}-, β_3-, or β_4-containing currents. As a general trend, AA did not effect $\tau_{INACT\text{-}slow}$ for β_{1b}-, β_3-, or β_4-containing currents (Fig. 8 B), although AA decreased $\tau_{INACT\text{-}slow}$ for currents with β_{1b} at +20 mV, β_{2a} at 0 and +20 mV, β_3 at +20 to +40 mV, and β_4 at 0 mV (n = 5–7; P < 0.05). Overall, $Ca_V1.3$ currents with β_{1b}, β_3, or β_4 appear to fast inactivate more rapidly in the presence of AA, consistent with the $r40$ data.

To measure the voltage sensitivity of holding potential–dependent inactivation, currents were normalized to peak inward current during the test pulse and plotted against the conditioning test potential (Fig. 8 C). The CTL inactivation curve for $Ca_V1.3$ currents with β_{2a} was shifted ~10 mV more positive than the other $Ca_V\beta$ subunits. From fits to the Boltzmann equation (Fig. 8 C), we found that AA had no effect on the $V_{inact}1/2$ of the $Ca_V1.3$ currents coexpressed with β_{1b} (CTL, −41.1 ± 1.2 mV; AA, −44.1 ± 0.8 mV), β_{2a} (CTL, −29.8 ± 0.7 mV; AA, −30.4 ± 0.8 mV), β_3 (CTL, −38.5 ± 0.8 mV; AA, −41.9 ± 1.1 mV), or β_4 (CTL, −38.5 ± 0.8 mV; AA, −40.8 ± 0.4 mV). Similar values for CTL $Ca_V1.3$ β_3 $V_{inact}1/2$ have been reported (Scholze et al., 2001). These results show that AA has no effect on the voltage dependence of holding potential–dependent inactivation for $Ca_V1.3$ currents with any $Ca_V\beta$ subunit.

Closer inspection of the $Ca_V1.3$ inactivation curves for β_{1b}-, β_3-, or β_4-containing channels revealed that inactivation occurred at negative test potentials before channels began to open, suggesting that channels were inactivating from a closed state similar to T- (Frazier et al., 2001) and N-type Ca^{2+} channels (Patil et al., 1998). For example, at the conditioning pulse of −60 mV, ~10–15% of the channels were inactivated even though the channels do not open at this voltage. At the conditioning pulse of −90 mV, only 5% of the channels were inactivated. The slope between −100 and −60 mV, before channels begin to activate, does not appear to be an artifact or an accumulation of inactivation because testing longer intervals between the final test pulse and the following conditioning pulse had no effect on the voltage dependence of the inactivation curves with and without AA (not depicted). Regardless, this observed inactivation profile does not change in the presence of AA.

Although the voltage sensitivity did not shift after AA, significantly fewer β_{2a}-containing channels were available to open per voltage (−10 to +50 mV) in the presence of AA (Fig. 8 C). This finding correlates with the amount of current remaining at the end the 2.2-s conditioning pulse ($r2200$). Here, AA had no effect on the $r2200$ for β_{1b}-, β_3-, or β_4-containing channels because >90% of CTL and inhibited current had already undergone fast inactivation. However, AA decreased the $r2200$ for β_{2a}-containing channels (Fig. 8 A, inset in box).

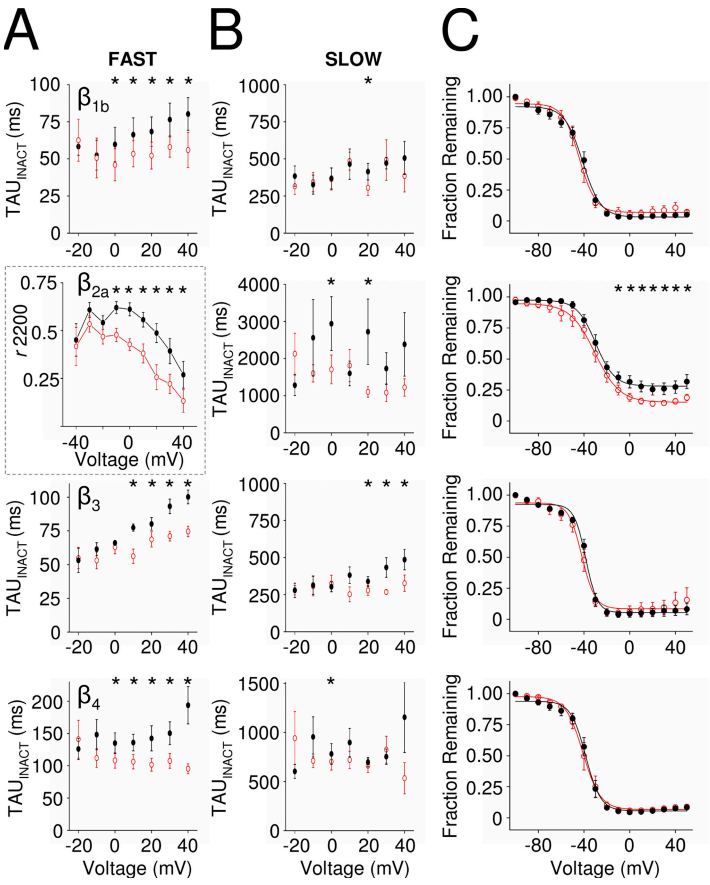

Figure 8. Holding potential–dependent inactivation curves for $Ca_V1.3b$ are unaffected by AA. (A and B) Time constants for inactivation were measured at each voltage for CTL (filled circle) or 10 µM AA (open circle) from a holding potential of −60 mV. Currents from β_{1b}-, β_3-, and β_4-containing channels were best fit with two exponentials, τ_{fast} (A) and τ_{slow} (B). Currents from β_{2a}-containing channels were best fit with one exponential, τ_{slow} (n = 5–7; *, P < 0.05). (C) Currents were normalized to maximal inward current during the 40-ms test pulse after a 2.2-s conditioning pulse and plotted against the conditioning pulse voltage. Curves were fit to the Boltzmann equation. Conditions are the same as A and B. (Inset in box) Current remaining at the end of the conditioning pulse for $Ca_V1.3b$, β_{2a} currents ($r2200$; from Fig. 7, A and C) was divided by the peak inward current and plotted against the voltage of the conditioning pulse (filled circle, CTL; open circle, AA; n = 13; *, P < 0.05).

Therefore, over a longer time scale, currents with β_{2a} subunits also displayed more inactivation in the presence of AA. By decreasing the number of channels available to open during a given test pulse, fast inactivation of β_{1b}-, β_3-, or β_4-containing channels was accentuated, whereas holding potential–dependent inactivation of β_{2a}-containing channels was accentuated by AA. Thus, AA may act via a common mechanism of stabilizing deep closed states independently of which $Ca_V\beta$ subunit is coexpressed with $Ca_V1.3b$.

Because an apparent increase in channels residing in closed conformations could be due to an increase in recovery time from the inactivated state, we next examined recovery from inactivation using two separate protocols. First, peak current was measured every 5 s after the inactivation protocol in the absence and presence of AA (Fig. 9 A). Current recoveries were fit to a single exponential time constant and did not significantly differ between CTL and AA for $Ca_V1.3$ with any $Ca_V\beta$ subunit (Fig. 9 B). Second, in another test for changes in recovery from inactivation, the test pulse was placed at various time points (Δt) after a 1-s conditioning pulse (Fig. 9 C). In this protocol, we chose a 1-s conditioning pulse to +20 mV based on where maximal holding potential inactivation occurred (Fig. 8 C, β_3). Recovery from inactivation was best fitted with two time constants: $\tau_1 = 291$ ms and $\tau_2 = 13.6$ s. Recovery from inactivation in the presence of AA also was best fitted with two time constants: $\tau_1 = 371$ ms and $\tau_2 = 17.2$ s (Fig. 9 D). This experiment allowed for the measurement of recovery from fast inactivation, which was overlooked in fitting the recovery from the time courses during which currents were evoked every 5 s (Fig. 9, A and B). Consistent with the first protocol, the time constants were not significantly different between CTL and AA (Fig. 9 D). However, the fractional amplitudes A_1 and A_2 associated with the recovery time constants revealed an important difference. The CTL values for A_1 and A_2 were 0.52 and 0.34, respectively, whereas the values for AA were 0.67 and 0.18, respectively. The finding suggests that in the presence of AA, there are more channels recovering from fast inactivation and fewer channels recovering from slow inactivation. Therefore, AA does not change the rate constant between inactivated and closed conformations, but rather alters the number of channels recovering from fast and holding potential–dependent inactivation.

Magnitude of AA inhibition of β_{2a}-containing channels is independent of fast inactivation

β_{2a} uniquely stands apart from other $Ca_V\beta$ subunits because it contains two palmitoyl groups at cysteine residues in the N terminus (Chien et al., 1996), conferring unique non-inactivating properties to Ca_V current (Qin et al., 1998). To test whether the non-inactivating properties of β_{2a}-containing channels are responsible for less AA inhibition, we tested another β_2 splice variant, β_{2e}, which is not palmitoylated, yet still has non-inactivating

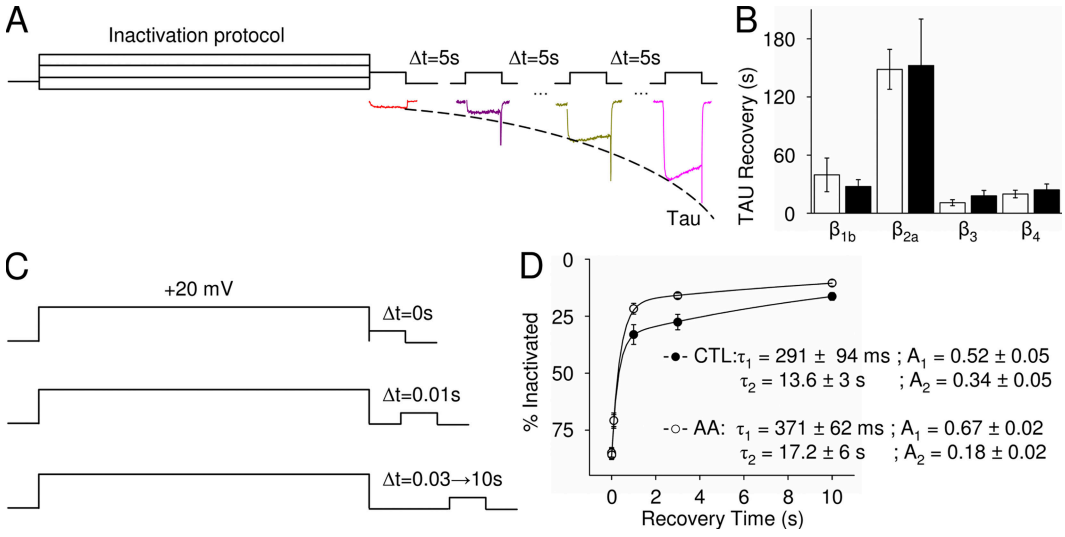

Figure 9. Recovery from inactivation for $Ca_V1.3b$ is unaffected by AA. (A) Schematic of protocol for recovery from inactivation. Peak inward current was measured at 0 s and every 5 s after the inactivation protocol (Fig. 7) for CTL or in the presence of 10 μM AA. The time constant for recovery from holding potential–dependent inactivation (TAU) was fit to the current amplitude plotted over time (dashed line). (B) Summary bar graph of recovery from inactivation from A (open bars, CTL; filled bars, AA). Recovery was best fitted with one exponential ($n = 5$–7). (C) Second protocol for recovery from inactivation. Currents were inactivated during a 1-s conditioning pulse to +20 mV. At various time points ($\Delta t = 0$, 0.01, 0.1, 0.3, 3, 1, and 10 s), a 40-ms test pulse to −10 mV was placed. Recovery was fit to the current amplitude from the test pulse plotted against the interpulse time interval. (D) Fits for recovery from inactivation for $Ca_V1.3b$, β_3 currents from the protocol described in C. Recoveries under CTL conditions (filled circle) or in the presence of AA (open circle) were best fit by two exponentials. (Inset) Values representing time to recover and the distribution of current recovering from fast (τ_1, A_1) and slow (τ_2, A_2) inactivation ($n = 4$).

properties. After exposure to AA for 1 min, β_{2e} channels were inhibited 24 ± 8% (n = 6; P ≥ 0.26 compared with β_{2a}) (Fig. 10 A). Even though percent inhibition by AA approximately doubled for β_{2e} compared with β_{2a}, the difference was not significant. Therefore, we tested a β_{2a} subunit in which amino acid residues 3 and 4 have been mutated from cysteines to serines (β_{2a} C3,4S) resulting in a β_{2a} subunit that cannot be palmitoylated (Restituito et al., 2000). After exposure to AA for 1 min, β_{2a} C3,4S channels were inhibited 32 ± 5% (n = 6; P < 0.05 compared with β_{2a}) (Fig. 10 A). To examine whether the loss of the palmitoyl groups or the loss of non-inactivating properties resulted in more inhibition by AA, we tested a β_{2a} C3,4S subunit with a CD8 sequence attached. CD8 is a transmembrane protein, and thus attaching CD8 to the N terminus of β_{2a} C3,4S restores the non-inactivating properties (Restituito et al., 2000). After exposure to AA for 1 min, β_{2a} C3,4S-CD8 channels were inhibited 44 ± 9% (n = 9; P < 0.05 compared with β_{2a}) (Fig.10 A). Fig. 10 B shows the r40 for currents with β_{2e}, β_{2a} C3,4S, and β_{2a} C3,4S-CD8 before and after AA application. Representative sweeps for each condition are displayed in Fig. 10 C. β_{2e} and β_{2a} C3,4S-CD8 currents both display non-inactivating properties yet are inhibited more by AA than β_{2a} channels, suggesting that the palmitoyl groups of β_{2a}, and not the non-inactivating properties, are responsible for decreased AA inhibition of $Ca_V1.3b$.

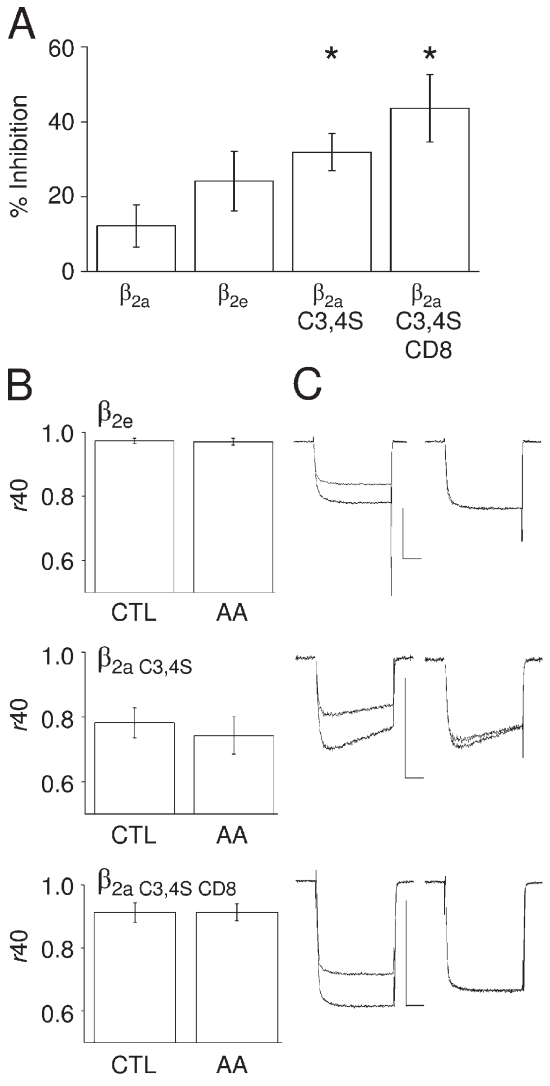

Figure 10. Magnitude of AA inhibition of β_{2a}-containing channels is independent of fast inactivation. (A) Summary bar graphs of percent inhibition of $Ca_V1.3b$ currents with β_{2a} (from Fig. 3 A for comparison), β_{2e}, depalmitoylated β_{2a} C3,4S, and depalmitoylated β_{2a} C3,4S-CD8 (n = 6–9; *, P < 0.05 compared with β_{2a}). (B) The amount of inactivation, measured as r40, for β_{2e}, depalmitoylated β_{2a} C3,4S, and depalmitoylated β_{2a} C3,4S-CD8 before (CTL) and after a 1-min exposure to AA. (C) Representative current traces from $Ca_V1.3b$ coexpressed with β_{2e}, depalmitoylated β_{2a} C3,4S, and depalmitoylated β_{2a} C3,4S-CD8. (Left) Before (black) and after a 1-min exposure to AA (dark gray). (Right) Normalized to the end of the 40-ms test pulse. Bars, 1 nA, 10 ms.

Palmitoylation of β_{2a} interferes with AA inhibition

A compelling idea is that palmitoyl groups of β_{2a} may compete for a "fatty acid" or "AA" binding site on $Ca_V1.3$. Therefore, we tested if excess PA would block AA inhibition. A 1-min exposure to 10 µM PA inhibited β_{2a} C3,4S currents by 8 ± 4% (n = 3; P < 0.05 compared with 1 min exposure of β_{2a} C3,4S currents to 10 µM AA). Cells were then preincubated in 10 µM PA in Tyrode's solution before establishing a seal. After breakthrough, bath solution containing 10 µM PA was washed in and a baseline current was measured before adding 10 µM PA + 10 µM AA. After a 1-min exposure to 10 µM AA, currents were inhibited 11 ± 7% (n = 3; P < 0.05 compared with 1 min exposure of β_{2a} C3,4S currents to 10 µM AA). Fig. 11 A is a summary bar graph of mean inhibition by AA. Fig. 11 B shows representative sweeps for each condition. A summary bar graph for current remaining for each condition is shown in Fig. 11 C. Overall, these results suggest that the palmitoyl groups of β_{2a} or excess PA may compete with AA for an inhibitory site on $Ca_V1.3b$.

DISCUSSION

AA inhibits $Ca_V1.3b$ L-Ca^{2+} currents regardless of the $Ca_V\beta$ subunit

Here, we show that AA inhibits $Ca_V1.3b$, a short form of $Ca_V1.3$ with a truncated C terminus, ruling out its importance in modulation by AA. Because we had previously characterized AA's effects on native L-current from SCG neurons (Liu and Rittenhouse, 2000; Liu et al., 2001, 2006), we used $Ca_V1.3b$, which was cloned from SCG neurons (Xu and Lipscombe, 2001), in these studies. Using ETYA, a nonmetabolizable form of a fatty acid similar to AA, we show that inhibition and kinetic changes of $Ca_V1.3$ are due to AA itself, and not a metabolite (Figs. 4 and 6, D and E). Current inhibition occurs regardless of the $Ca_V\beta$ subunit coexpressed. However,

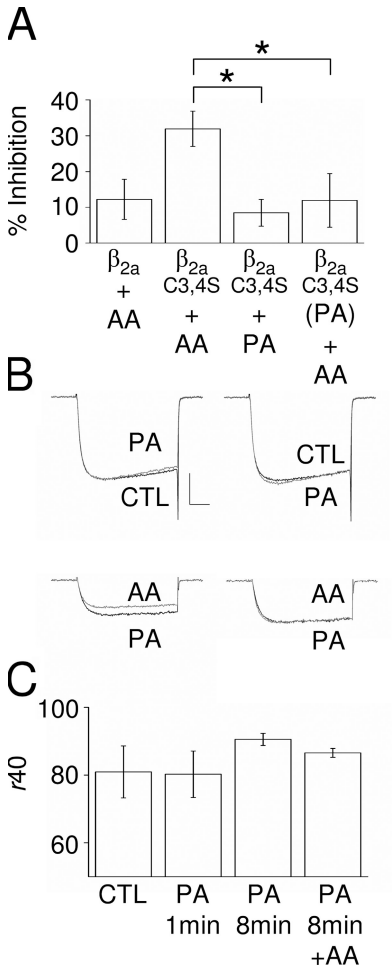

Figure 11. Palmitoylation of β_{2a} interferes with AA $Ca_V1.3b$ inhibition. (A) Summary bar graphs of percent inhibition of $Ca_V1.3b$ currents with β_{2a}, depalmitoylated β_{2a} C3,4S (from Fig. 10 A for comparison), β_{2a} C3,4S in the presence of 10 μM PA for 1 min, and β_{2a} C3,4S preincubated in 10 μM PA for at least 8 min, and then exposed to 10 μM PA + μM AA for 1 min (n = 3–4; *, $P < 0.05$ compared with β_{2a} C3,4S). (B) Representative current traces. (Left, top) $Ca_V1.3b$ coexpressed with depalmitoylated β_{2a} C3,4S before (CTL) and after exposure to 10 μM PA for 1 min. (Left, bottom) β_{2a} C3,4S preincubated with 10 μM PA for 8 min (PA), and the addition of 10 μM PA + 10 μM AA for 1 min (AA). (Right) Normalized to the end of the 40-ms test pulse. (C) Summary bar graphs of current remaining for each condition. Bars, 0.5 nA, 10 ms.

the magnitude of inhibition after 1 min by either AA or ETYA was less with coexpression of β_{2a} than β_{1b}, β_3, or β_4. In addition, AA decreased $r40$, a measure of fast inactivation, and TTP of channels containing β_{1b}, β_3, or β_4 (Figs. 1, 2, and 6). In contrast, β_{2a}-containing channels showed no differences in TTP after exposure to AA. These complex changes are manifested in the presence of AA due to the influence of different $Ca_V\beta$ subunits coexpressed with $Ca_V1.3b$ on gating kinetics. Because the kinetic changes do not correlate with percent inhibition by AA over time (Figs. 1 D and 3 C), AA may act at multiple sites on L-channels.

AA inhibits native L-current in a variety of systems: cardiac muscle (Petit-Jacques and Hartzell, 1996; Xiao et al., 1997; Liu, 2007), skeletal muscle T-tubule membranes (Oz et al., 2005), smooth muscle (Shimada and Somlyo, 1992), SCG (Liu and Rittenhouse, 2000; Liu et al., 2001), photoreceptors (Vellani et al., 2000), and retinal glial cells (Bringmann et al., 2001). No consensus of mechanism exists as to how AA inhibits L-channel activity, whether directly, through AA metabolites, or via AA activating a phosphatase. Varying effects of AA on L-current may be due to expression of different L-$Ca_V\alpha_1$ subunits. For example, ventricular myocytes and smooth muscle cells primarily express $Ca_V1.2$, whereas SCG neurons, atrial myocytes, and cochlear hair cells express $Ca_V1.3$ (Lin et al., 1996; Platzer et al., 2000; Mangoni et al., 2003; Catterall et al., 2005). Additionally, $Ca_V1.2$ and $Ca_V1.3$ undergo alternative splicing (Hell et al., 1993; Safa et al., 2001), which may contribute to the differences in L-current kinetics observed with varying cell types. Notably, the lack of AA-induced kinetic changes in cardiac myocytes and SCG neurons may be due to high levels of β_{2a} subunit mRNA found in these cells (Lin et al., 1996; Birnbaumer et al., 1998).

Current inhibition by AA does not require channels to open

In this study of whole cell recombinant $Ca_V1.3b$ L-current, we found changes induced by AA complementary to our previous single-channel data. Analysis of unitary L-channel gating in SCG neurons revealed that AA-induced inhibition had no effect on mean open time or on unitary current amplitude (Liu and Rittenhouse, 2000). Consistent with this finding, the results from three experiments indicate that the open conformation of $Ca_V1.3b$ is not necessary for inhibition by AA. First, test pulse length did not affect the magnitude of current inhibition by AA (Fig. 3 E). In fact, reducing the test pulse length increased the amount of AA-induced current inhibition. Second, β_{2a}-containing currents, which do not exhibit fast inactivation and therefore gate open and closed longer, exhibited less inhibition (Figs. 1–5). Third, $Ca_V1.3b$ channels exhibited robust inhibition when held closed for 1 min during AA application and then allowed to open (Fig. 3 E). Thus, AA does not confer inhibition by binding to the open state.

AA stabilizes a closed conformation of $Ca_V1.3b$

Single-channel analysis of L-current in SCG neurons also revealed that AA decreased channel open probability by increasing the number of null sweeps. Moreover, when channels were active, AA decreased the number of openings and increased first latency and mean closed time (Liu and Rittenhouse, 2000). Together, the changes in the unitary activity indicate that AA stabilizes L-channels in one or more nonconducting states: either closed or inactivated conformations.

We hypothesize that AA decreases channel availability by increasing the number of L-channels stabilized in a deep closed state, as opposed to an inactivated state, based on several findings. First, we observe more AA inhibition from channels held at a membrane potential of −90 mV than at −60 mV (Fig. 3, A and B); at a membrane potential of −90 mV, channels undergo less closed state inactivation than at −60 mV (Fig. 8 C, β_{1b}, β_3, and β_4). Second, the voltage sensitivity of holding potential–dependent inactivation does not change with AA (Fig. 8 C). Third, when measuring both fast and slow recovery for β_3-containing channels, we observe no change in recovery from inactivation in the presence of AA (Fig. 9), suggesting that the transition rate from inactivated to closed conformations remains unchanged. Moreover, inactivated channels regardless of voltage will not respond to positive test pulses until given enough time at a negative holding potential to recover. On the other hand, stabilizing a deep closed state would require more depolarized voltage and, hence, more time to transition the channel to an open state, consistent with increases in first latency (Liu and Rittenhouse, 2000). The first latency of 30 ms fits well with the notion that L-channels in SCG neurons couple to β_{2a}. Liu and Rittenhouse (2000) showed that in the presence of AA, this time increases to 90 ms. In these single-channel experiments, the effect of AA on a single channel's activity is directly monitored. Here, we hypothesize that when measuring whole cell current in the presence of AA, the observed current arises from channels not inhibited by AA.

Our hypothesis that AA modulates channels in deep, closed conformations, but not channels that are in a conformation near to the open state, is reminiscent of the two populations of channels described as willing and reluctant. Historically, willing-reluctant gating terminology has been used to describe gating that occurs when G proteins bind to high voltage–activated Ca^{2+} (Ca_V2) channels (Bean, 1989). G protein $G_{\beta\gamma}$ subunits can bind Ca_V2 α_1 subunits and inhibit Ca_V2 current by stabilizing "reluctant gating" conformations. This inhibition can be relieved by a strong depolarizing prepulse (typically to +120 mV), releasing the $G_{\beta\gamma}$ subunit and allowing the channel to occupy "willing gating" conformations. Although CTL $Ca_V1.3$ currents display facilitation after a strong depolarizing prepulse, the mechanism is not mediated by $G_{\beta\gamma}$ binding $Ca_V1.3$ (Bell et al., 2001; Safa et al., 2001) and remains unknown. Determining whether AA promotes facilitation under certain conditions as well as inhibition will require further detailed experimentation.

One versus two sites of AA action

More recently, the willing-reluctant terminology has been used to describe how PIP_2 increases channel availability of the Ca_V2 family (Wu et al., 2002; Gamper et al., 2004). PIP_2 has been hypothesized to act at two unidentified sites termed the "S" and "R" sites on Ca_V2 channels (Wu et al., 2002). When PIP_2 binds to the high affinity S site, channel activity is stabilized and whole cell currents are protected from rundown. When PIP_2 binds to the lower affinity R site, channels open more slowly during weak depolarizations, similar to the reluctant gating observed with G proteins (Wu et al., 2002; Michailidis et al., 2007). Exogenous application of AA appears to exert the opposite effects of PIP_2's dual actions on $Ca_V2.2$ channels where AA decreases current magnitude but increases the activation and inactivation kinetics (unpublished data). These two actions of AA are distinguishable both biophysically and pharmacologically (Barrett et al., 2001; Liu et al., 2001). Because AA is a product of PIP_2 breakdown by several phospholipases, these findings raise an interesting possibility that AA also acts at two analogous sites on $Ca_V1.3$ to antagonize PIP_2's putative actions on L-current (Michailidis et al., 2007). A similar bidirectional relationship between PIP_2 and AA has been documented for Kir and K_V channels in which PIP_2 and AA are hypothesized to act at distinct sites (Oliver et al., 2004; Tucker and Baukrowitz, 2008). Whether exogenously applied AA competitively displaces PIP_2 or acts directly or indirectly to alter a distinct site on $Ca_V1.3$ channels to elicit inhibition has not yet been determined; however, free AA interacting at the same location(s) of PIP_2's fatty acid tail(s) to confer inhibition is an appealing idea in its simplicity.

Activation kinetics of $Ca_V1.3b$ residual currents are faster in the presence of AA

In addition to current inhibition, AA decreases TTP and the τ_{ACT} becomes faster. We present the following scenario to explain our interpretation of this result. At rest, channels reside in a series of closed conformations whereby τ_{ACT} describes the rate of channels transitioning from different closed conformations to the open conformation: RC + WC→O. Under CTL conditions, RC channels may have PIP_2 bound to the R site as well as the S site (Wu et al., 2002), resulting in channels available to open but at a slower rate of transition to the open conformation than WC channels. However, the overall rate will be the average of RC + WC channels and is dependent on the proportion of channels occupying each closed conformation. If AA stabilizes a deep, closed conformation, RC channels, which transition through the closed states more slowly than WC channels, would be more susceptible to inhibition (Fig. 12 A). Thus, AA does not cause reluctant or willing gating, but rather AA is more likely to act on reluctant gating channels.

If AA selectively stabilizes RC channels in a closed state, making them unlikely to open during a test pulse, only the WC channels, with the faster activation rate, will open and determine the whole cell current kinetics.

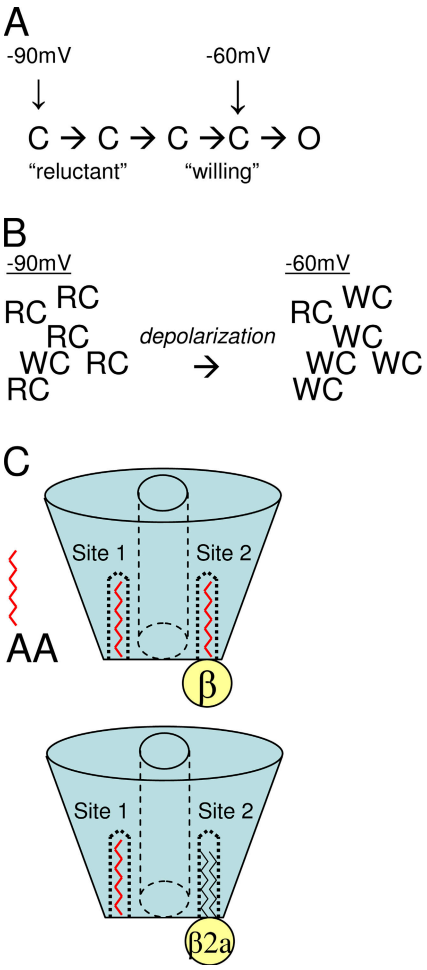

Figure 12. Models for $Ca_V1.3b$ current inhibition by AA. (A) Schematic for a single channel undergoing different closed conformations before opening. Conformations in deep closed states, like those at −90 mV, may preferentially bind AA. (B) Schematic for whole cell channel populations. Two populations of channels may exist at a given holding potential. At −90 mV, the majority of channels are in RC conformations as opposed to WC conformations. At −60 mV, the majority of channels are in WC conformations. AA preferentially binding RC channels may explain the greater amount of AA inhibition at −90 mV. (C) Hypothetical model for the inhibition of $Ca_V1.3b$ channels by AA. (Top) $Ca_V1.3b$ channel with two sites for AA inhibition. (Bottom) The palmitoyl groups of β_{2a} (or excess PA) may occlude one of the sites for AA inhibition.

The decreases in TTP (i.e., peak inward current occurs faster) after exposure to AA is consistent with this model. Notably, in experiments with β_{2a}-containing channels, TTP changes are not observed with 40-ms test pulses as this time frame is not long enough to account for the changes in activation; however, TTP changes are observed for β_{2a} in the 2.2-s pulses that are long enough to account for first latency changes from 30 to 90 ms observed in SCG neurons. In several experiments, the membrane potential was held at −60 mV, near the threshold for opening (−50 mV) for $Ca_V1.3$ (Xu and Lipscombe, 2001). At this voltage, more channels would be predicted to reside in conformations closer to the open state. We observed less inhibition at −60 mV than with a holding potential of −90 mV, at which a greater percentage of channels would reside in deeper closed conformations (Fig. 12 B). Thus, in the presence of AA, the observed smaller current with a faster τ_{ACT} arises from willing channels residing closer to the open state and "above" the closed state(s) stabilized by AA. It will be interesting to confirm these kinetic changes produced by AA for each of the subunit combinations in future studies of single-channel gating.

AA inhibits non-inactivating channels and accentuates $Ca_V\beta$ subunit–dependent inactivation kinetics of $Ca_V1.3b$ currents

To address whether AA stabilizes inactivated as well as closed conformations, we measured whole cell $Ca_V1.3$ currents under various inactivation protocols in the absence and presence of AA. Although $r40$ decreased for β_{1b}-, β_3-, and β_4-containing channels, the difference current was relatively non-inactivating. Because $Ca_V1.3$, β_{2a} currents only undergo slow inactivation, the decrease in $r2200$ revealed that there is a common mechanism for inhibition by AA that occurs regardless of the β subunit that is coexpressed. AA may preferentially inhibit the RC population of channels, and thus for β_{2a}-containing channels, the contribution of reluctant gating channels undergoing slow inactivation is decreased. Therefore, the percentage of WC channels, which remain available to open and available to undergo inactivation, is greater in the normalized holding potential–dependent inactivation curves. These findings suggest that when $Ca_V1.3b$ exhibits willing gating, L-channels will be less susceptible to inhibition by AA. Taken together, AA decreases the contribution of reluctant gating channels to the whole cell current, resulting in an increased proportion of the remaining current displaying inactivation kinetics of willing channels. Moreover, a shift in percentage of willing versus reluctant channels is manifested in the current kinetics in a $Ca_V\beta$ subunit–dependent manner after AA; fast inactivation increases for β_{1b}-, β_3-, and β_4-containing channels, whereas holding potential–dependent inactivation increases for β_{2a}-containing channels.

β_{2a} palmitoylation or excess PA decreases $Ca_V1.3b$ current inhibition by AA

Why is less inhibition of $Ca_V1.3b$ current observed after 1 min with AA for channels coexpressed with β_{2a}? One possibility is that the site of inhibition by AA occurs on the $Ca_V\alpha_1$ subunit. In this case, the palmitoylated β_{2a} may alter the conformation of the channel to noncompetitively regulate the availability of an AA binding pocket. Second, residues in the S6 transmembrane domains affect inactivation, suggesting an overall change in the pore structure (Stotz et al., 2004), a concept that has been compared with pore collapse or C-type inactivation

describing slow inactivation in Na^+ and K^+ channels (Lopez et al., 1994; Ogielska et al., 1995; Vilin et al., 1999). Channels coassembled with β_{2a} have a higher open probability than β_{1b} or β_3 (Colecraft et al., 2002) and would provide greater access for AA to contact these pore residues, promoting greater holding potential–dependent inactivation at more depolarized voltages.

Indeed, AA, or molecules with AA moieties in their structure including anandamide, can occupy the binding site for L-channel agonists and antagonists, such as dihydropyridines (DHPs) (Shimasue et al., 1996; Jarrahian and Hillard, 1997). DHPs interact with several critical amino acid residues in the pore of $Ca_V1.2$ and $Ca_V1.3$ (Sinnegger et al., 1997; Wappl et al., 2001; Liu et al., 2003; Yamaguchi et al., 2003). Thus, pore residues overlapping with the DHP site may constitute a site for AA interaction. However, if AA interacted with pore residues, coexpression of $Ca_V1.3b$ with β_{2a} should increase rather than decrease the magnitude of $Ca_V1.3$ current inhibition by AA. Alternatively, slow open-channel pore block by AA is a third possible mechanism of inhibition that would explain an increase in the rate of inactivation as well as a decreased TTP. This possibility seems unlikely because AA inhibits channels held closed in the absence of test potentials. Regardless, a role for $Ca_V\beta$ subunits modulating the AA site, whether by occupying a DHP site in the pore or by pore block, is plausible because these accessory subunits can fine-tune the affinity of L-channel blockers (Hering, 2002).

A fourth possibility is that two sites of AA action could exist, and either the palmitoyl group(s) or the inability of β_{2a} to fast inactivate prevents AA interaction with $Ca_V1.3$. In fact, the time course of inhibition of $Ca_V1.3b$, β_{2a} currents appears slower than with the other $Ca_V\beta$ subunits (Fig. 1 E, top), suggesting that palmitoylated β_{2a} may antagonize AA binding. Our findings suggest that the palmitoyl groups of β_{2a} either directly or indirectly impede AA's ability to inhibit channel activity (Figs. 10 and 11). We propose a model whereby two AA modulatory or fatty acid sites exist on $Ca_V1.3b$. We have included two sites in our model based on a previous determination that AA inhibited T-channels with a Hill coefficient of 1.6 (Talavera et al., 2004). T-channel expression requires no other accessory subunit, suggesting that at least two sites of interaction exist on $Ca_V\alpha$ subunits. When $Ca_V1.3b$ colocalizes with β_{1b}, β_3, or β_4, both sites are available. When $Ca_V1.3b$ colocalizes with β_{2a}, the palmitoyl groups interfere or occupy at least one of the sites, resulting in less inhibition by AA (Fig. 12 C).

Possible physiological implications

$Ca_V1.3$ channels colocalize with large-conductance Ca^{2+}-activated K^+ channels (BK channels) in the brain (Grunnet and Kaufmann, 2004). Increases in AA levels may directly affect Ca^{2+}-activated K^+ channel activity, resulting in an enhancement of K^+ current (Denson et al., 2000; Clarke et al., 2002; Sun et al., 2007). The influence of AA on Ca^{2+} influx and K^+ efflux, as well as several other ion channels (Meves, 2008), could profoundly alter membrane excitability. Additionally, proteins with two adjacent palmitoyl groups, such as β_{2a}, may localize to cholesterol-rich microdomains (Pike, 2003), which may in turn alter $Ca_V1.3$ susceptibility to modulation by AA.

In certain pathophysiological conditions, such as ischemia and stroke, concentrations of AA, comparable to those used in the present study, are released in the brain (Lipton, 1999). Brain regions with high expression of β_{2a} subunits (Birnbaumer et al., 1998; McEnery et al., 1998) may be less affected by the cytotoxic effects of AA release downstream of neurotransmitter activation because β_{2a}-containing $Ca_V1.3b$ currents show less inhibition. Conversely, AA could increase cell survival by inhibiting Ca^{2+} influx because large sustained influxes of Ca^{2+}, such as that of the non-inactivating β_{2a} current, can be cytotoxic (Lipton, 1999). Similarly, currents from β_{1b}-, β_3-, or β_4-containing $Ca_V1.3b$ channels show more AA inhibition; this overall depression of Ca^{2+} influx may decrease excitotoxicity. Whether AA acts indirectly or by binding to $Ca_V1.3b$ or the $Ca_V\beta$ subunit remains unanswered. Because AA is hydrophobic, if inhibition is due to a direct binding effect, $Ca_V1.3$ with its 24 membrane–spanning segments seems the more likely candidate as opposed to the cytosolic $Ca_V\beta$ subunit. Future studies involving mutational analyses of $Ca_V\alpha$ or the $Ca_V\beta$ subunits should provide these answers.

The authors would like thank Liwang Liu, John Heneghan, and Tora Mitra-Ganguli for their assistance and discussions; TzuFeng Chung for maintaining the HEK M1 cell line; and José Lemos, William Kobertz, Haley Melikian, Elizabeth Luna, and Edward Perez-Reyes for thoughtful critique of the manuscript.

This work was supported by National Institutes of Health grants (NS34195 and NS07366) and funding from UMASS Medical School.

Lawrence G. Palmer served as editor.

Submitted: 19 May 2008
Accepted: 11 March 2009

REFERENCES

Arias, J.M., J. Murbartian, I. Vitko, J.H. Lee, and E. Perez-Reyes. 2005. Transfer of beta subunit regulation from high to low voltage-gated Ca2+ channels. *FEBS Lett.* 579:3907–3912.

Axelrod, J., R.M. Burch, and C.L. Jelsema. 1988. Receptor-mediated activation of phospholipase A2 via GTP-binding proteins: arachidonic acid and its metabolites as second messengers. *Trends Neurosci.* 11:117–123.

Banihashemi, B., and P.R. Albert. 2002. Dopamine-D2S receptor inhibition of calcium influx, adenylyl cyclase, and mitogen-activated protein kinase in pituitary cells: distinct Galpha and Gbetagamma requirements. *Mol. Endocrinol.* 16:2393–2404.

Bannister, R.A., K. Melliti, and B.A. Adams. 2002. Reconstituted slow muscarinic inhibition of neuronal (Ca(v)1.2c) L-type Ca2+ channels. *Biophys. J.* 83:3256–3267.

Barrett, C.F., L. Liu, and A.R. Rittenhouse. 2001. Arachidonic acid reversibly enhances N-type calcium current at an extracellular site. *Am. J. Physiol. Cell Physiol.* 280:C1306–C1318.

Bean, B.P. 1989. Neurotransmitter inhibition of neuronal calcium currents by changes in channel voltage dependence. *Nature.* 340:153–156.

Bell, D.C., A.J. Butcher, N.S. Berrow, K.M. Page, P.F. Brust, A. Nesterova, K.A. Stauderman, G.R. Seabrook, B. Nurnberg, and A.C. Dolphin. 2001. Biophysical properties, pharmacology, and modulation of human, neuronal L-type (alpha(1D), Ca(V)1.3) voltage-dependent calcium currents. *J. Neurophysiol.* 85:816–827.

Birnbaumer, L., N. Qin, R. Olcese, E. Tareilus, D. Platano, J. Costantin, and E. Stefani. 1998. Structures and functions of calcium channel beta subunits. *J. Bioenerg. Biomembr.* 30:357–375.

Brandt, A., J. Striessnig, and T. Moser. 2003. CaV1.3 channels are essential for development and presynaptic activity of cochlear inner hair cells. *J. Neurosci.* 23:10832–10840.

Brandt, A., D. Khimich, and T. Moser. 2005. Few CaV1.3 channels regulate the exocytosis of a synaptic vesicle at the hair cell ribbon synapse. *J. Neurosci.* 25:11577–11585.

Bringmann, A., S. Schopf, F. Faude, and A. Reichenbach. 2001. Arachidonic acid-induced inhibition of Ca2+ channel currents in retinal glial (Muller) cells. *Graefes Arch. Clin. Exp. Ophthalmol.* 239:859–864.

Cardenas, C.G., L.P. Del Mar, and R.S. Scroggs. 1997. Two parallel signaling pathways couple 5HT1A receptors to N- and L-type calcium channels in C-like rat dorsal root ganglion cells. *J. Neurophysiol.* 77:3284–3296.

Catterall, W.A. 2000. Structure and regulation of voltage-gated Ca2+ channels. *Annu. Rev. Cell Dev. Biol.* 16:521–555.

Catterall, W.A., E. Perez-Reyes, T.P. Snutch, and J. Striessnig. 2005. International Union of Pharmacology. XLVIII. Nomenclature and structure-function relationships of voltage-gated calcium channels. *Pharmacol. Rev.* 57:411–425.

Chavis, P., H. Shinozaki, J. Bockaert, and L. Fagni. 1994. The metabotropic glutamate receptor types 2/3 inhibit L-type calcium channels via a pertussis toxin-sensitive G-protein in cultured cerebellar granule cells. *J. Neurosci.* 14:7067–7076.

Chien, A.J., K.M. Carr, R.E. Shirokov, E. Rios, and M.M. Hosey. 1996. Identification of palmitoylation sites within the L-type calcium channel beta2a subunit and effects on channel function. *J. Biol. Chem.* 271:26465–26468.

Clarke, A.L., S. Petrou, J.V. Walsh Jr., and J.J. Singer. 2002. Modulation of BK(Ca) channel activity by fatty acids: structural requirements and mechanism of action. *Am. J. Physiol. Cell Physiol.* 283:C1441–C1453.

Colecraft, H.M., B. Alseikhan, S.X. Takahashi, D. Chaudhuri, S. Mittman, V. Yegnasubramanian, R.S. Alvania, D.C. Johns, E. Marban, and D.T. Yue. 2002. Novel functional properties of Ca(2+) channel beta subunits revealed by their expression in adult rat heart cells. *J. Physiol.* 541:435–452.

Day, M., P.A. Olson, J. Platzer, J. Striessnig, and D.J. Surmeier. 2002. Stimulation of 5-HT(2) receptors in prefrontal pyramidal neurons inhibits Ca(v)1.2 L type Ca(2+) currents via a PLCbeta/IP3/calcineurin signaling cascade. *J. Neurophysiol.* 87:2490–2504.

Denson, D.D., X. Wang, R.T. Worrell, and D.C. Eaton. 2000. Effects of fatty acids on BK channels in GH(3) cells. *Am. J. Physiol. Cell Physiol.* 279:C1211–C1219.

Frazier, C.J., J.R. Serrano, E.G. George, X. Yu, A. Viswanathan, E. Perez-Reyes, and S.W. Jones. 2001. Gating kinetics of the α1I T-type calcium channel. *J. Gen. Physiol.* 118:457–470.

Gamper, N., V. Reznikov, Y. Yamada, J. Yang, and M.S. Shapiro. 2004. Phosphatidylinositol 4,5-bisphosphate signals underlie receptor-specific Gq/11-mediated modulation of N-type Ca2+ channels. *J. Neurosci.* 24:10980–10992.

Gao, L., L.A. Blair, G.D. Salinas, L.A. Needleman, and J. Marshall. 2006. Insulin-like growth factor-1 modulation of CaV1.3 calcium channels depends on Ca2+ release from IP3-sensitive stores and calcium/calmodulin kinase II phosphorylation of the alpha1 subunit EF hand. *J. Neurosci.* 26:6259–6268.

Grunnet, M., and W.A. Kaufmann. 2004. Coassembly of big conductance Ca2+-activated K+ channels and L-type voltage-gated Ca2+ channels in rat brain. *J. Biol. Chem.* 279:36445–36453.

Hell, J.W., R.E. Westenbroek, C. Warner, M.K. Ahlijanian, W. Prystay, M.M. Gilbert, T.P. Snutch, and W.A. Catterall. 1993. Identification and differential subcellular localization of the neuronal class C and class D L-type calcium channel alpha 1 subunits. *J. Cell Biol.* 123:949–962.

Hering, S. 2002. beta-Subunits: fine tuning of Ca(2+) channel block. *Trends Pharmacol. Sci.* 23:509–513.

Hering, S., S. Berjukow, S. Sokolov, R. Marksteiner, R.G. Weiss, R. Kraus, and E.N. Timin. 2000. Molecular determinants of inactivation in voltage-gated Ca2+ channels. *J. Physiol.* 528:237–249.

Jarrahian, A., and C.J. Hillard. 1997. Arachidonylethanolamide (anandamide) binds with low affinity to dihydropyridine binding sites in brain membranes. *Prostaglandins Leukot. Essent. Fatty Acids.* 57:551–554.

Jones, S.W., and K.S. Elmslie. 1997. Transmitter modulation of neuronal calcium channels. *J. Membr. Biol.* 155:1–10.

Kobrinsky, E., K.J. Kepplinger, A. Yu, J.B. Harry, H. Kahr, C. Romanin, D.R. Abernethy, and N.M. Soldatov. 2004. Voltage-gated rearrangements associated with differential beta-subunit modulation of the L-type Ca(2+) channel inactivation. *Biophys. J.* 87:844–857.

Koschak, A., D. Reimer, I. Huber, M. Grabner, H. Glossmann, J. Engel, and J. Striessnig. 2001. alpha 1D (Cav1.3) subunits can form l-type Ca2+ channels activating at negative voltages. *J. Biol. Chem.* 276:22100–22106.

Lazarewicz, J.W., E. Salinska, and J.T. Wroblewski. 1992. NMDA receptor-mediated arachidonic acid release in neurons: role in signal transduction and pathological aspects. *Adv. Exp. Med. Biol.* 318:73–89.

Lin, Z., C. Harris, and D. Lipscombe. 1996. The molecular identity of Ca channel alpha 1-subunits expressed in rat sympathetic neurons. *J. Mol. Neurosci.* 7:257–267.

Lipton, P. 1999. Ischemic cell death in brain neurons. *Physiol. Rev.* 79:1431–1568.

Liu, G., N. Dilmac, N. Hilliard, and G.H. Hockerman. 2003. Ca v 1.3 is preferentially coupled to glucose-stimulated insulin secretion in the pancreatic beta-cell line INS-1. *J. Pharmacol. Exp. Ther.* 305:271–278.

Liu, L., and A.R. Rittenhouse. 2000. Effects of arachidonic acid on unitary calcium currents in rat sympathetic neurons. *J. Physiol.* 525:391–404.

Liu, L., C.F. Barrett, and A.R. Rittenhouse. 2001. Arachidonic acid both inhibits and enhances whole cell calcium currents in rat sympathetic neurons. *Am. J. Physiol. Cell Physiol.* 280:C1293–C1305.

Liu, L., R. Zhao, Y. Bai, L.F. Stanish, J.E. Evans, M.J. Sanderson, J.V. Bonventre, and A.R. Rittenhouse. 2006. M1 muscarinic receptors inhibit L-type Ca2+ current and M-current by divergent signal transduction cascades. *J. Neurosci.* 26:11588–11598.

Liu, S.J. 2007. Inhibition of L-type Ca2+ channel current and negative inotropy induced by arachidonic acid in adult rat ventricular myocytes. *Am. J. Physiol. Cell Physiol.* 293:C1594–C1604.

Lopez, G.A., Y.N. Jan, and L.Y. Jan. 1994. Evidence that the S6 segment of the Shaker voltage-gated K+ channel comprises part of the pore. *Nature.* 367:179–182.

Mangoni, M.E., B. Couette, E. Bourinet, J. Platzer, D. Reimer, J. Striessnig, and J. Nargeot. 2003. Functional role of L-type Cav1.3 Ca2+ channels in cardiac pacemaker activity. *Proc. Natl. Acad. Sci. USA.* 100:5543–5548.

Marks, T.N., and S.W. Jones. 1992. Calcium currents in the A7r5 smooth muscle-derived cell line. An allosteric model for calcium channel activation and dihydropyridine agonist action. *J. Gen. Physiol.* 99:367–390.

McEnery, M.W., C.L. Vance, C.M. Begg, W.L. Lee, Y. Choi, and S.J. Dubel. 1998. Differential expression and association of calcium

channel subunits in development and disease. *J. Bioenerg. Biomembr.* 30:409–418.

Meves, H. 2008. Arachidonic acid and ion channels: an update. *Br. J. Pharmacol.* 155:4–16.

Michailidis, I.E., Y. Zhang, and J. Yang. 2007. The lipid connection-regulation of voltage-gated Ca(2+) channels by phosphoinositides. *Pflugers Arch.* 455:147–155.

Ogielska, E.M., W.N. Zagotta, T. Hoshi, S.H. Heinemann, J. Haab, and R.W. Aldrich. 1995. Cooperative subunit interactions in C-type inactivation of K channels. *Biophys. J.* 69:2449–2457.

Oliver, D., C.C. Lien, M. Soom, T. Baukrowitz, P. Jonas, and B. Fakler. 2004. Functional conversion between A-type and delayed rectifier K+ channels by membrane lipids. *Science.* 304:265–270.

Olson, P.A., T. Tkatch, S. Hernandez-Lopez, S. Ulrich, E. Ilijic, E. Mugnaini, H. Zhang, I. Bezprozvanny, and D.J. Surmeier. 2005. G-protein-coupled receptor modulation of striatal CaV1.3 L-type Ca2+ channels is dependent on a Shank-binding domain. *J. Neurosci.* 25:1050–1062.

Oz, M., A. Alptekin, Y. Tchugunova, and M. Dinc. 2005. Effects of saturated long-chain N-acylethanolamines on voltage-dependent Ca2+ fluxes in rabbit T-tubule membranes. *Arch. Biochem. Biophys.* 434:344–351.

Patil, P.G., D.L. Brody, and D.T. Yue. 1998. Preferential closed-state inactivation of neuronal calcium channels. *Neuron.* 20:1027–1038.

Pemberton, K.E., and S.V. Jones. 1997. Inhibition of the L-type calcium channel by the five muscarinic receptors (m1-m5) expressed in NIH 3T3 cells. *Pflugers Arch.* 433:505–514.

Peralta, E.G., A. Ashkenazi, J.W. Winslow, J. Ramachandran, and D.J. Capon. 1988. Differential regulation of PI hydrolysis and adenylyl cyclase by muscarinic receptor subtypes. *Nature.* 334:434–437.

Petit-Jacques, J., and H.C. Hartzell. 1996. Effect of arachidonic acid on the L-type calcium current in frog cardiac myocytes. *J. Physiol.* 493:67–81.

Pike, L.J. 2003. Lipid rafts: bringing order to chaos. *J. Lipid Res.* 44:655–667.

Platzer, J., J. Engel, A. Schrott-Fischer, K. Stephan, S. Bova, H. Chen, H. Zheng, and J. Striessnig. 2000. Congenital deafness and sinoatrial node dysfunction in mice lacking class D L-type Ca2+ channels. *Cell.* 102:89–97.

Qin, N., D. Platano, R. Olcese, J.L. Costantin, E. Stefani, and L. Birnbaumer. 1998. Unique regulatory properties of the type 2a Ca2+ channel beta subunit caused by palmitoylation. *Proc. Natl. Acad. Sci. USA.* 95:4690–4695.

Restituito, S., T. Cens, C. Barrere, S. Geib, S. Galas, M. De Waard, and P. Charnet. 2000. The [beta]2a subunit is a molecular groom for the Ca2+ channel inactivation gate. *J. Neurosci.* 20:9046–9052.

Safa, P., J. Boulter, and T.G. Hales. 2001. Functional properties of Cav1.3 (alpha1D) L-type Ca2+ channel splice variants expressed by rat brain and neuroendocrine GH3 cells. *J. Biol. Chem.* 276:38727–38737.

Scholze, A., T.D. Plant, A.C. Dolphin, and B. Nurnberg. 2001. Functional expression and characterization of a voltage-gated CaV1.3 (alpha1D) calcium channel subunit from an insulin-secreting cell line. *Mol. Endocrinol.* 15:1211–1221.

Serrano, J.R., E. Perez-Reyes, and S.W. Jones. 1999. State-dependent inactivation of the α1G T-type calcium channel. *J. Gen. Physiol.* 114:185–201.

Shimada, T., and A.P. Somlyo. 1992. Modulation of voltage-dependent Ca channel current by arachidonic acid and other long-chain fatty acids in rabbit intestinal smooth muscle. *J. Gen. Physiol.* 100:27–44.

Shimasue, K., T. Urushidani, M. Hagiwara, and T. Nagao. 1996. Effects of anandamide and arachidonic acid on specific binding of (+) -PN200-110, diltiazem and (-) -desmethoxyverapamil to L-type Ca2+ channel. *Eur. J. Pharmacol.* 296:347–350.

Singer, D., M. Biel, I. Lotan, V. Flockerzi, F. Hofmann, and N. Dascal. 1991. The roles of the subunits in the function of the calcium channel. *Science.* 253:1553–1557.

Sinnegger, M.J., Z. Wang, M. Grabner, S. Hering, J. Striessnig, H. Glossmann, and J. Mitterdorfer. 1997. Nine L-type amino acid residues confer full 1,4-dihydropyridine sensitivity to the neuronal calcium channel alpha1A subunit. Role of L-type Met1188. *J. Biol. Chem.* 272:27686–27693.

Stotz, S.C., S.E. Jarvis, and G.W. Zamponi. 2004. Functional roles of cytoplasmic loops and pore lining transmembrane helices in the voltage-dependent inactivation of HVA calcium channels. *J. Physiol.* 554:263–273.

Sun, X., D. Zhou, P. Zhang, E.G. Moczydlowski, and G.G. Haddad. 2007. Beta-subunit-dependent modulation of hSlo BK current by arachidonic acid. *J. Neurophysiol.* 97:62–69.

Takahashi, S.X., J. Miriyala, and H.M. Colecraft. 2004. Membrane-associated guanylate kinase-like properties of beta-subunits required for modulation of voltage-dependent Ca2+ channels. *Proc. Natl. Acad. Sci. USA.* 101:7193–7198.

Talavera, K., M. Staes, A. Janssens, G. Droogmans, and B. Nilius. 2004. Mechanism of arachidonic acid modulation of the T-type Ca^{2+} channel α1G. *J. Gen. Physiol.* 124:225–238.

Tang, X., E.M. Edwards, B.B. Holmes, J.R. Falck, and W.B. Campbell. 2006. Role of phospholipase C and diacylglyceride lipase pathway in arachidonic acid release and acetylcholine-induced vascular relaxation in rabbit aorta. *Am. J. Physiol. Heart Circ. Physiol.* 290:H37–H45.

Tucker, S.J., and T. Baukrowitz. 2008. How highly charged anionic lipids bind and regulate ion channels. *J. Gen. Physiol.* 131:431–438.

Vellani, V., A.M. Reynolds, and P.A. McNaughton. 2000. Modulation of the synaptic Ca2+ current in salamander photoreceptors by polyunsaturated fatty acids and retinoids. *J. Physiol.* 529:333–344.

Vilin, Y.Y., N. Makita, A.L. George Jr., and P.C. Ruben. 1999. Structural determinants of slow inactivation in human cardiac and skeletal muscle sodium channels. *Biophys. J.* 77:1384–1393.

Wappl, E., J. Mitterdorfer, H. Glossmann, and J. Striessnig. 2001. Mechanism of dihydropyridine interaction with critical binding residues of L-type Ca2+ channel alpha 1 subunits. *J. Biol. Chem.* 276:12730–12735.

Wikstrom, M.A., S. Grillner, and A. El Manira. 1999. Inhibition of N- and L-type Ca2+ currents by dopamine in lamprey spinal motoneurons. *Neuroreport.* 10:3179–3183.

Wu, L., C.S. Bauer, X.G. Zhen, C. Xie, and J. Yang. 2002. Dual regulation of voltage-gated calcium channels by PtdIns(4,5)P2. *Nature.* 419:947–952.

Xiao, Y.F., A.M. Gomez, J.P. Morgan, W.J. Lederer, and A. Leaf. 1997. Suppression of voltage-gated L-type Ca2+ currents by polyunsaturated fatty acids in adult and neonatal rat ventricular myocytes. *Proc. Natl. Acad. Sci. USA.* 94:4182–4187.

Xu, W., and D. Lipscombe. 2001. Neuronal Ca(V)1.3alpha(1) L-type channels activate at relatively hyperpolarized membrane potentials and are incompletely inhibited by dihydropyridines. *J. Neurosci.* 21:5944–5951.

Yamaguchi, S., B.S. Zhorov, K. Yoshioka, T. Nagao, H. Ichijo, and S. Adachi-Akahane. 2003. Key roles of Phe1112 and Ser1115 in the pore-forming IIIS5-S6 linker of L-type Ca2+ channel alpha1C subunit (CaV 1.2) in binding of dihydropyridines and action of Ca2+ channel agonists. *Mol. Pharmacol.* 64:235–248.

Yehuda, S., S. Rabinovitz, R.L. Carasso, and D.I. Mostofsky. 1998. Fatty acids and brain peptides. *Peptides.* 19:407–419.

Zhang, H., Y. Fu, C. Altier, J. Platzer, D.J. Surmeier, and I. Bezprozvanny. 2006. Ca1.2 and CaV1.3 neuronal L-type calcium channels: differential targeting and signaling to pCREB. *Eur. J. Neurosci.* 23:2297–2310.

Zhang, Y., L.L. Cribbs, and J. Satin. 2000. Arachidonic acid modulation of alpha1H, a cloned human T-type calcium channel. *Am. J. Physiol. Heart Circ. Physiol.* 278:H184–H193.